

2021-2022

Master Agronomie, Environnement, Territoires, Paysage, Forêt (AETPF)

Major Forests and their Environment

Global tree distribution disequilibrium dynamics:
View of land-use transformation and paleoclimate anomaly

PENGCHENG LAI

Master thesis, defended at Nancy on August 31, 2022

Supervisor: Josep M. Serra-Diaz, Associate Professor, AgroParisTech
Academic referent: Jean-Claude Gégout, Full Professor, AgroParisTech

Abstract: Understanding tree species distribution is a critical conservation priority in ecosystem restoration and the post-2020 goals for biodiversity protection. Recent studies have evidenced that past climate changes have shaped current tree species distribution through mechanisms of extirpation, migration and persistence, evidencing that the present-day species distribution is not in equilibrium with the current climate (e.g., climate disequilibrium). Likewise, the present-day climate change has caused species migration and habitat distribution shifts. However, little is known about how the effects of past and present land-use change constraint current species distribution. Here, we combined global datasets of prehistorical and historical land use on forest cover and human land use intensity with the current climate and paleoclimate changes (Late Miocene and Last Glacial Maximum) to holistically understand how these factors affect the disequilibrium of current tree species distribution. We calculated the range unfilling – unoccupied area but climatically suitable – for 19,041 tree distributions across seven realms to understand global species disequilibrium. Range unfilling was calculated as the ratio between the potential climatic range which has not been occupied – based on niche models – and current species geographical occupancy – using the alpha-hulls method. Our results highlight the significant impacts of land-use conversion and paleoclimate anomaly on present-day tree species distribution, with effects of past versus present land use and climate varies evidently across biogeographic realms. Over recent centuries, the dramatic negative effect of intensified land-use conversion on tree species distribution recalls the urgent need to protect key biodiversity areas.

Keywords: climatic disequilibrium; human pressure; land use; paleoclimate legacies; range unfilling; species distribution; tree cover

Contents

INTRODUCTION	1
MATERIALS AND METHODS	2
Tree Species Selection and Occurrence Records	2
Realized Species Ranges.....	2
Environmental Data.....	3
Potential Climatic Range Determination.....	4
Calculation of Range Unfilling	5
Spatial and Statistical Analysis	6
Data Availability.....	6
RESULTS.....	6
Geographic Distribution and Species Distribution Modeling.....	6
Range Unfilling and its Distribution Status at Each Realm.....	7
Impact of Land-use Transformation and Climate Anomaly on Range Unfilling.....	7
DISCUSSION.....	9
Range Unfilling	9
Land-use Conversions Predictors of Range Unfilling.....	10
Paleoclimate Anomaly Predictors of Range Unfilling.....	11
Other Explanations.....	13
CONCLUSION	13
ACKNOWLEDGEMENTS	13
REFERENCE	14
ANNEX	18

INTRODUCTION

Numerous studies have revealed that prior human societies and paleoclimate have significantly impacted current terrestrial ecosystems (1-3). Regardless of this emerging evidence, a joint understanding of past anthropogenic activities and paleoclimate anomalies are often missing in species distribution studies (4, 5). However, there is a widespread recognition that the current geographical distribution of any given species is shaped not simply by recent land use and anthropogenic climate change but by historical land-use transformation and paleoclimate change (3, 6-8). This impact could be especially prevalent in the case tree species (3, 9, 10).

High rates of past and current climatic changes are hypothesized to exceed the capacity of many tree species to migrate with the climate, which leads to mismatches between climatic conditions and climatic preferences for the species present in the community (11) – e.g., disequilibrium between species distribution and climate. Ultimately, this may lead to areas climatically suitable not being occupied by the species (range unfilling). Range unfilling (RU) is indeed present in North American and European tree species (12-14), but it is not the case for plant species' RU in China, which may be due to methodological differences (15). Despite a relatively well understanding of the effects of post-quaternary dispersal limitation, paleoclimate, and current climate on species' geographic distribution in the Northern Hemisphere, the impact of these factors is rarely discovered on the distribution of tree species in other biomes.

Land use impacts on tree species distribution are evident at regional to continental scales. In many landscapes, historical human activities have become one of the most important factors in favoring some plants, including tree species, to increase their geographical distribution via

propagation, domestication, and cultivation (1, 2). In contrast, extinction risks were also elevated for others by land-use change and habitat loss (16-18). However, evidence for the impacts of land-use changes during critical prehistorical and historical periods on species ranges on the global scale is limited. We still lack an understanding of how historical and prehistorical land-use changes affected current species distribution for all the forest ecosystems across seven major realms.

We address this knowledge gap by analyzing RU in response to factors associated with past land-use change and climate anomalies on a global scale. Here, RU is calculated as the ratio between the potential (climatic) geographic range – identified through species distribution models, and the current distribution range – identified through occurrence records and geographic algorithms, as an index to measure how well species have occupied their potential ranges. In this study, we question (A): what is the global tree disequilibrium status quo across seven major biogeographical realms?; and (B) Do land use changes in critical prehistorical and historical periods and paleoclimate anomalies drive current tree disequilibrium?

We hypothesized that the potential ranges of global tree species are potentially wide unfilled (hypothesis a), which is consistent with tree species' range unfilling in Europe and North America (12, 13). We also hypothesized that present-day tree species distribution is co-influenced by the current climate, current land use, paleoclimate change, and (pre-)historical land-use change (hypothesis b). Assuming that land use changes in the early stages (early agricultural era and agricultural era) of civilization development should predispose tree species to be benefited from human activities, whereas rapidly shifting from cultured anthropogenic biome (anthromes) or

wildlands to intensive anthromes in recent centuries could hinder tree species from filling more of their potential geographic distribution (1, 2). Indeed, land use has been closely associated with key biodiversity areas, species richness, and threatened species richness since pre-history until the Columbian exchange and European colonial expansion, and the strength of this relation in many regions declined after 1500 CE (1, 19). This assumption has not been examined under the context of the impact of land-use changes on range unfilling. Despite current climate and post-quaternary dispersal constraints that could explain some variation of range unfilling (12-14), little is known about the impact of paleoclimate change from the realm to the globe for tree species. We, therefore, explore how the Late Miocene climate (Miocene, 11.6 - 7.2 mya) and Last Glacial Maximum (LGM, ~21 kya) climate change shaped tree species distribution across seven major realms.

We evaluate current tree disequilibrium globally (Fig. 3 A) and in each realm (Fig. 3 B & C). Here, we analyze the importance of paleoclimate change, current climate, past land-use transformation, and current land use on present-day tree species distribution globally and for seven major realms. Our results indicate the current tree species distribution is co-shaped by present-day human pressure, current climate, and sometimes to a larger extent, legacies of prehistorical and historical anthropogenic impacts and paleoclimatic change.

MATERIALS AND METHODS

Tree Species Selection and Occurrence Records

We obtained the records from the global tree species checklist [GlobalTreeSearch; GTS (20)] and standardized the taxonomic names with the Taxonomic Name Resolution Service (21). The GTS applied the tree definition agreed by the International Union

for Conservation of Nature's Global Tree Specialist Group: a woody plant with usually a single stem growing to a height of at least two meters, or if multi-stemmed, then at least one vertical stem five centimeters in diameter at breast height (20). A preliminary list of 57,958 tree species was chosen.

We compiled occurrence records for tree species from the most comprehensive and public accessible occurrence database: the Global Biodiversity Information Facility (GBIF; <https://www.gbif.org/>, accessed on December 20, 2021). Due to the well-known issues of errors and biases in this global species occurrence database (22), we employed a workflow to integrate, assess and control the data quality of occurrence records (23) for initially 52,168 tree species. This workflow performs two main tests to exclude problematic records and improve data quality. The species occurrence data was cleaned with the CoordinateCleaner package [v.2.0.20, (24)], and the list of tree species was down to 51,620, with an average occurrence per species of 515.

Realized Species Ranges

Alpha hulls were then used to construct the geographic range of each tree species with 10 or more unique occurrence records using the *getDynamicAlphaHull* function of the rangeBuilder package [v.1.6, (25)]. Alpha hulls are a widely used technique to delimit species' geographic ranges with either convex or concave internal angles (26). We discarded species with less than 10 unique occurrence records or with fragmented occurrence records across disjunct realms as they either cannot build a reliable realized range or some of their occurrences are outside of the native ranges (species names can be found in the species list). This results in 29,166 tree species. *InitialAlpha* and *fraction* arguments in the *getDynamicAlphaHull* function were set to 3 and 0.95 by default, while we allowed a maximum number of 5 disjunct polygons. Alpha levels were increased until meeting

both the fraction and partCount conditions (25), resulting in alpha degrees of 43 on average. We then rasterize the estimated geographic distribution maps to 9.8×9.8 -km, a similar resolution used in the historical land-use study (1), using the terra package [v.1.5.34, (27)]. Although compared with other used techniques such as convex hull, the alpha hull shows explicit improvement in the temporal and spatial distribution of sampling effort and spatial accuracy (26). It may still overestimate the species' actual area of occupancy and thus should be considered as an estimate of the extent of occurrence [Fig. 2 C, (28)].

Environmental Data.

We downloaded current climate variables (1981-2010 averages) from the Chelsa 2.1 database (www.chelsa-climate.org) at a resolution of 30 arcsec, including 19 bioclimatic variables [bio1 to bio19, (29)]. Based on expert knowledge, bio1(mean annual temperature, MAT), bio5(mean daily maximum temperature of the warmest month) to bio14(precipitation of the driest month), bio16(mean monthly precipitation of the wettest quarter) to bio19(mean monthly precipitation amount of the coldest quarter) were chosen and used in species distribution modeling to project current species' suitable climatic space. Current MAT (bio1) and current mean annual precipitation (bio12, MAP) were also used to calculate climate anomalies for the Quaternary paleoclimatic change.

Given the limited availability of paleoclimate data, we incorporated two bioclimatic predictors commonly used in related studies: mean annual temperature and mean annual precipitation (15, 30). Two paleoecological epochs were selected, ranging from ~11.6 - 7.2 Mya to ~21 Kya, reflecting warmer or colder climatic conditions than the current climate. Specifically, the Miocene refers to a warmer

climate compared to the present (31, 32). Climatic data of the Miocene were extracted from the Late Miocene vegetation reconstruction study at a resolution of 150 arcsec (32). The LGM was used to reflect global cooling events (33). We retrieved the LGM climate from the Chelsa paleoclimate database (<https://chelsa-climate.org/chelsa-trace21k/>) at a resolution of 30 arcsec (34). The Miocene climate anomalies were calculated as differences between the Miocene climate predictors and the LGM climate predictors, while the LGM climate anomalies were calculated as differences between the LGM climate and the current climate (from 1981 to 2010). Current MAT and MAP were also selected to explain climatic disequilibrium of tree species despite the current climate having been used in predicting species' potential geographical distribution, thus to some degree already included in the calculation of RU.

Besides paleoclimate, RU was also affected by land use and its transformation during several critical historical periods. The *anthropogenic biome DGG baseline* database was used to map global land use over the past 12,000 years from 10 Kya to 2017 CE (1). Based on Anthromes maps, we used Human Modification (HM) index (35) and Tree Cover [TC, (36)] with their alterations in explaining variations of species RU for five critical land-use periods, namely the Early Agricultural Era (EAE, 10,000 BCE to 1 CE), Agricultural Era (AE, 1 CE to 1500 CE), Era of Discovery (ED, 1500 CE to 1850 CE), Era of Post-First Industrial Revolution (EPFIR, 1850 CE to 1950 CE) and Era of Post-Second Industrial Revolution (EPSIR, 1950 CE to 2013 CE). The HM map was calculated based on modeling 13 global-scale anthropogenic stressors with 2016 CE as a median year, many of which highly impact biodiversity and ecosystem services (35). The tree cover database shows global tree cover at the peak of the growing season in 2010 CE (36). Values of HM and TC are both ranging from 0 to 1. The median year of HM

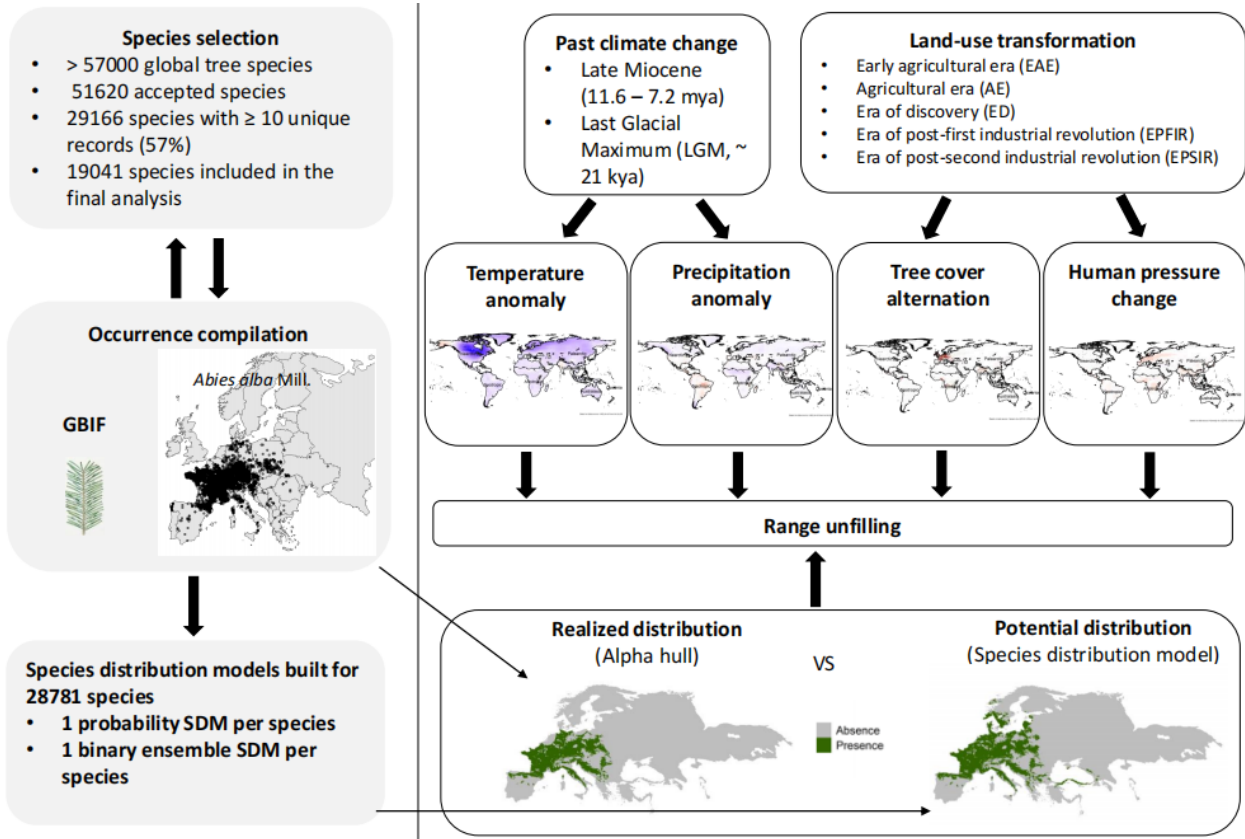


FIGURE 1 The workflow of this study was used to determine the impact of key land-use transformation eras and paleoecological epochs. Range unfilling: calculated as the ratio of the potential range, which has not been occupied to geographic distribution space overlapped with the potential range. A detailed demonstration for calculating range unfilling can be found in Figure 2.

and TC 2013 CE was chosen to project land use conversion during EPSIR.

We extracted median values of current TC and HM for each anthrome category (Annex Fig. 4 & 5) and assigned these values to TC and HM based on the anthrome class for each designated year. HM and TC alteration was calculated by HM and TC difference between two designated years. The median values of predictors of climate anomaly and land use were extracted with the same resolution of the Anthrome DGG system [$\sim 96 \text{ km}^2$; median value = 96.19 km^2 (1)] and then rasterized to $9.8 \times 9.8\text{-km}$ Eckert IV equal-area projection using the exactextractr [v.0.8.2, (37)] and terra package (27).

Potential Climatic Range Determination

To simulate the potential climatic geographical range for tree species, we applied species distribution models (SDMs) using the Range Bagging algorithm (38). Range Bagging uses presence-only data and models species range boundaries in multiple dimensions of climatic space using ensemble modeling, namely bootstrap aggregation (38). The models were projected with 15 current climate variables to the ecoregion(s) where occurrence records present and its adjacent ecoregions and classified into presence/absence with the threshold of the 5% scores of the testing dataset. For validation, we used 80% of random-partitioned species occurrence records to train the Range

Bagging models, and performance was evaluated with the area under the ROC (receiver operating characteristic curve) or AUC (39) on the remaining test dataset and a similar-sized random set of background points. To further select Range Bagging models with good performances, we additionally calculated the continuous Boyce index (CBI), a reliable measure designed for presence-only data prediction (40), using the enmSdm package [v.0.9.3, (41)]. Those models with both AUC and CBI ≥ 0.8 passed the evaluation, and a total of 19041 species were selected for further analysis.

Calculation of Range Unfilling

For each species (19,041 species), RU – interpreted here as a measure of climatic disequilibrium – was calculated as the ratio of the potential range (SDM), which has not

been occupied to geographic distribution space (alpha hull) (Fig. 2 C, species RU list available at R research compendium). We only count the areas where estimates of geographic range overlapped with the potential ranges as the current geographic range when we calculate RU (conservative RU). Nevertheless, alternative approaches such as RU (alpha-hull) calculated as the ratio of potential range and the complete geographic range were highly correlated with conservative RU selected here (0.91, Annex Fig. 2). Both geographic distribution and potential range space were calculated as the number of grid cells at the resolution of 9.8×9.8 -km. The global tree species filling map was calculated as the ratio of the number of species present estimated by the alpha-hull method to the number of species predicted as present by the range bagging algorithm at the 300 arcsec resolution.

TABLE 1 Predictors, with their abbreviations, are used to explain the variation of range unfilling in this study.

Predictor	Abbreviation
Current tree cover	TC
Current human pressure (indicated by the human modification index)	HM
Tree cover change during the early agricultural era	TC-EAE
Human pressure change during the early agricultural era	HM-EAE
Tree cover change during the agricultural era	TC-AE
Human pressure change during the agricultural era	HM-AE
Tree cover change during the era of discovery	TC-ED
Human pressure change the era of discovery	HM-ED
Tree cover change during the era of post-first industrial revolution	TC-EPFIR
Human pressure change during the era of post-first industrial revolution	HM-EPFIR
Tree cover change during the era of post-second industrial revolution	TC-EPSIR
Human pressure change during the era of post-second industrial revolution	HM-EPSIR
Current mean annual temperature	MAT
Current mean annual precipitation	MAP
Miocene temperature anomaly	MTA
Miocene precipitation anomaly	MPA
Last Glacial Maximum temperature anomaly	LGMTA
Last Glacial Maximum precipitation anomaly	LGMPA

Spatial and Statistical Analysis

We analyzed the influence of land use transformation and climate anomaly on RU. Explanatory variables included current tree cover and human pressure and its alteration during five critical land-use periods (TC, HM, TC-EAE, HM-EAE, TC-AE, HM-AE, TC-ED, HM-ED, TC-EPFIR, HM-EPFIR, TC-EPSIR, HM-EPSIR), Miocene temperature anomaly (MTA), Miocene precipitation anomaly (MPA), LGM temperature anomaly (LGMTA), LGM precipitation anomaly (LGMPA), MAT and MAP (Fig. 1, Tab. 1). The environmental variables were extracted at mean values across species potential climatic geographical ranges.

We examined global tree species' current RU status and its distribution in each realm (Fig. 3). RU was classified into five classes: extremely low (class1, $0 < RU \leq 0.5$), low (class2, $0.5 < RU \leq 1$), moderate (class3, $1 < RU \leq 4$), high (class4, $4 < RU \leq 37$), extremely high (class5, $37 < RU$). One-third of the potential geographic range was unfilled when RU equals 0.5, while 1 represents an identical amount of potential geographic space unfilled versus filled. 4 and 37 were selected as they were 50% and 95% quantile of RU, respectively. Kruskal-Wallis test (42) was used to compare the difference between the mean RU of each realm and the mean RU of global tree species by only including extremely low to high range unfilling ($RU \leq 37$).

RU follows a lognormal distribution; therefore, the response variable is log-transformed in the following statistical analysis. To control the bias in data mobilization and social-economic differences, and variances of biogeographical history between realms (43), we fitted a Generalized Linear Mixed Model (GLMM) with the realms as a random effect to explain the variance of RU for the 19041 tree species. Further analyses were done on seven major

realms with the explanatory variables standardized in Generalized linear models (GLMs). Due to multicollinearity concerns, an explanatory variable was removed from the GLMM and GLMs if the variance inflation factor (VIF) was above 10 (44). A slightly higher VIF (e.g., more than 5) is considered an inadequate reason to exclude one variable (45). VIF values of GLMs and GLMM can be found in the R research compendium. Extreme values of explanatory variables were removed based on Cook's distance (46). We mainly focused on the explanatory variables which have significant importance (p value < 0.05) and impact (coefficient value $\neq 0$) on RU in our study.

Data Availability

All other supplementary information which not included in the annex can be accessible as an R research compendium on Github (<https://github.com/pengchenglai/Tree-disequilibrium>). The whole study was done using R [v.4.1.1,(47)].

RESULTS

Geographic Distribution and Species Distribution Modeling

Alpha hulls estimated geographic ranges for 28,683 tree species and 376 species built with convex hulls because they failed to meet the criteria (see materials and methods). This species list was then used to model their potential range, and a total number of 28,781 SDMs were built, with 19,041 passing the model evaluation (accessible in the R research compendium). The average AUC and BIC of these 19,041 SDMs are 0.92 and 0.93 (Annex Fig. 3). Fig. 2 shows an example of range estimation in geographic distribution and potential range of *Abies alba* Mill. and calculation of its range unfilling at the resolution of $9.8 \times 9.8\text{-km}$.



FIGURE 2 Range estimation and range unfilling of *Abies alba* Mill.: A. Realized range estimated by alpha-hull; and B. potential climatic distribution built based upon range bagging. C. Range unfilling: calculated as the ratio of the potential range, which has not been occupied (showed in blue), to the geographic distribution space that overlapped with the potential range (showed in green).

Range Unfilling and its Distribution Status at Each Realm

On average, species' potential ranges are 10.7 times larger than their geographic ranges, while the median RU of global tree species is 4 (Fig. 3 A). Species with moderate to extremely high RU ($1 < \text{RU}$) were around 85.9% globally (Fig. 3 A), indicating that potential ranges were widely unfilled for most tree species. This proportion is even higher in Neotropic (93.8%), Afrotropic (92.1%), Oceania (87.7%), and Indomalayan (87%) (Fig. 3 B, see Annex Fig. 1 for biological realms map). This phenomenon can also be observed and confirmed in the global tree species range filling map: tree species have poorly occupied vast land areas in Neotropic and Afrotropic (Fig. 4). Even by excluding extremely high RU ($\text{RU} > 37$), all median values of RU were lower than their mean values, presenting a substantial number of species with high RU (between 4 and 37) exist in each realm. Results of the Kruskal-Wallis test have shown that the potential geographic range of tree species, on average, is significantly unfilled in Neotropic (7.57) and Afrotropic (6.75) compared with the mean RU of global tree species (6.24). In contrast, species in Palearctic (5.48), Indomalayan (4.88), Australasia (3.48), and Nearctic (2.82) significantly filled more of their potential ranges in comparison with the global average.

Impact of Land-use Transformation and Climate Anomaly on Range Unfilling

Land-use transformation and climate anomaly with current climate and land use can explain the 65.6% variance of range unfilling by incorporating realm as a covariate. Considering all tree species, current HM significantly reduces range unfilling, whereas tree cover has no significant impact (Tab. 2). From the early agricultural era to the agricultural era, the increase of human activities has favored tree species to occupy their potential geographical range more. In contrast, HM has had a positive effect on RU since the era of discovery, and it has become more influential in the latest era of post-second industrial revolution (Tab. 2). Similar to the impact of HM, TC change has a significantly negative relation with RU between the agricultural era and the era of discovery and the increase of TC begins to significantly hindered tree species from expanding their potential geographic ranges after the beginning of the post-first industrial revolution (Tab. 2). MAT has shown a significant impact for species: with higher temperatures, species could take more geographic space of their potential range, while MAP has a significantly positive relation on RU (Tab. 2). Despite its significant importance to RU, Miocene climate anomaly and LGM precipitation merely impact global trees' distribution (Tab. 2). However, the LGM temperature anomaly has reduced climatic disequilibrium with the

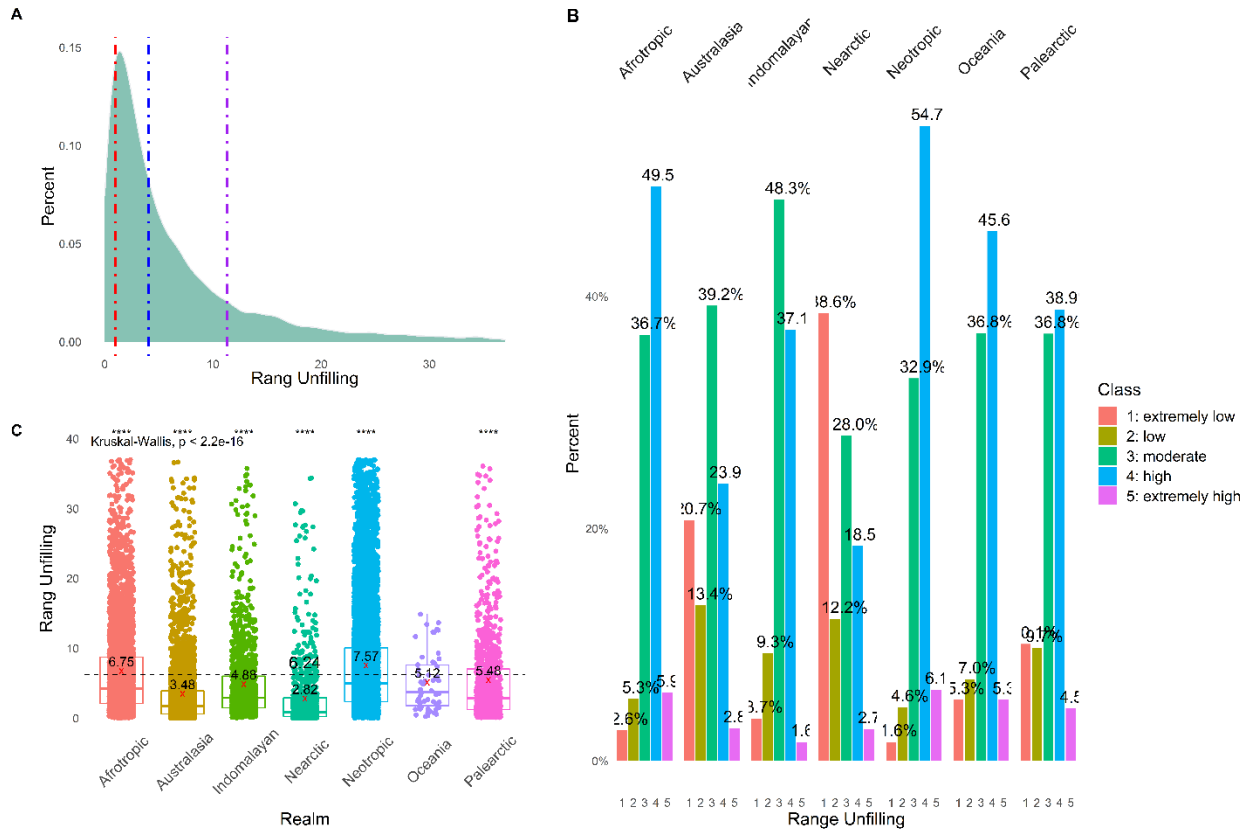


FIGURE 3 A. Global tree range unfilling density plot: the red vertical line indicates the boundary ($\text{RU} = 1$) between low and median range unfilling; the blue vertical line indicates the median RU (4.0) of all tree species; the purple vertical line indicates the mean RU (10.7) of all tree species. B. Tree range unfilling in each realm. Five RU classes: extremely low (class1, $0 < \text{RU} \leq 0.5$), low (class2, $0.5 < \text{RU} \leq 1$), moderate (class3, $1 < \text{RU} \leq 4$), high (class4, $4 < \text{RU} \leq 37$), extremely high (class5, $37 < \text{RU}$). C. Tree range unfilling in each realm compared with the mean RU of the global. Extremely high RU was removed for the simplicity and visualization of the comparison. The horizontal line indicates the mean value of the global tree species RU . The red cross represents the mean RU in each realm. The significance of the Kruskal-Wallis test is shown in the asterisk.

higher temperature difference between the LGM and current to fill more of their potential ranges.

Although the influence of land-use transformation and climate anomaly on RU have generally followed global patterns, different impacts between predictors and RU may exist in each realm (Tab. 3). For instance, despite their minor influences on global tree species, the LGM precipitation anomaly and Miocene precipitation anomaly significantly increased RU in Palearctic. In contrast, the Miocene temperature anomaly has reduced

RU in Neotropic, Afrotropic, and Indomalayan. We found that the relative impact of past and present land use and climate on RU vary greatly across realms (Tab. 3). In the Neotropic, we found prehistorical and historical land-use conversions, current climate, and Miocene temperature anomaly were the overall most critical predictors and left significant effects on current tree distribution. For Afrotropical forest ecosystems, range unfilling was mainly influenced by human activities during the era of post-first industrial revolution, current temperature, and Miocene

temperature anomaly. In the Australasia realm, human activities since the era of discovery were overwhelmingly the most important factor for RU, while Miocene temperature anomaly and human activities during the agricultural era and era of discovery predominantly impact present-day tree distribution in Indomalayan. RU of tree species in the Palearctic was primarily affected by land-use transformation after the post-industrial revolution, current temperature, LGM precipitation anomaly, and Miocene precipitation anomaly. In the Nearctic realm, RU was influenced mainly by the land-use transformation in the latest era and early stages. Besides the similar impact of HM change on RU during the agricultural era, the LGM temperature anomaly also plays a role in shaping the current tree distribution in Oceania.

DISCUSSION

Range Unfilling

We found that the potential ranges of global tree species are broadly unfilled, with a mean range unfilling of 10.7 (Fig. 3 A). Even for the average highest occupancy in Nearctic, species' potential ranges which have not been occupied are 5.5 times larger than their

estimated realized ranges (data not shown). These results are consistent with prior studies on European and North American trees, thus supporting hypothesis a: a widespread global disequilibrium for tree species.

Surprisingly, tree species in Neotropic(7.57) and Afrotropic(6.75) have significant higher RU compared with the global average without considering extreme high RU (>37), whereas species' potential ranges are only 4.9 times larger than their geographic ranges in Indomalayan on average (Figure 3 C). This result could be partially derived from the issue of unequal sampling effort regardless of improving data quality by cleaning. For instance, occurrence records from the GBIF have been repeatedly reported as biased to sites with higher altitudes, herbarium, and population density (43, 48, 49). This unequal sampling effort and problematic records could even be prevalent in some biogeographical regions [Annex Fig. 1, (48, 50, 51)]. Indeed, even by removing extreme high RU (>37), the mean RU is 2.8 in the Nearctic, which is more than two times higher compared with the study of the North American tree [1.1, (12)]. We remove species occurrence records outside of the country where their native ranges persist to avoid invasive species based on the specie

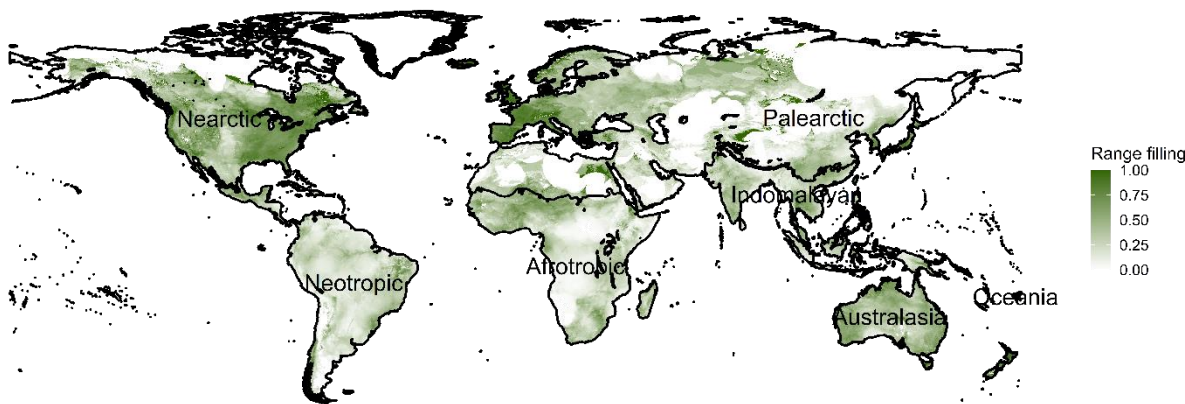


FIGURE 4 Global tree species range filling map, calculated as the ratio of the number of species present estimated by the alpha hull to the number of species predicted by SDM as present (realms indicated by lines).

TABLE 2 Results of the generalized linear mixed models of Range Unfilling. The significance of the P value is shown in bold. The complete name of predictors can be found in Table 2.

Predictors	Range unfilling	
	Estimates	P Value
Intercept	1.46 (0.43 – 2.49)	0.005
TC	0.00 (-0.00 – 0.00)	0.549
HM	-0.75 (-0.76 – -0.75)	<0.001
TC-EPSIR	0.01 (0.01 – 0.02)	<0.001
HM-EPSIR	4.76 (4.76 – 4.76)	<0.001
TC-EPFIR	0.01 (0.01 – 0.01)	<0.001
HM-EPFIR	0.50 (0.50 – 0.51)	<0.001
TC-ED	-0.01 (-0.02 – -0.01)	<0.001
HM-ED	2.02 (2.02 – 2.02)	<0.001
TC-AE	-0.04 (-0.04 – -0.04)	<0.001
HM-AE	-3.28 (-3.28 – -3.28)	<0.001
TC-EAE	0.00 (-0.00 – 0.00)	0.083
HM-EAE	-1.06 (-1.06 – -1.06)	<0.001
MAP	0.11 (0.11 – 0.12)	<0.001
MAT	-0.01 (-0.02 – -0.01)	<0.001
LGMPA	0.00 (0.00 – 0.00)	0.025
LGMIA	-0.15 (-0.15 – -0.15)	<0.001
MPA	0.00 (0.00 – 0.01)	<0.001
MTA	0.00 (0.00 – 0.00)	0.004
Random Effects		
σ^2	1019.30	
$\tau_{00 \text{ realm}}$	1945.23	
ICC	0.66	
N _{realm}	7	
Observations	19041	
Marginal R ² / Conditional R ²	0.000 / 0.656	

checklist from the GTS (20), although this approach could result in underestimating realized species ranges. Despite it probably due to the differences in sample size and methodologies, we could not run out the impact of uneven sample collections for the calculation of range unfilling; thus, it could be potentially overestimated globally. Further studies, therefore, should incorporate various sources of occurrence databases to model species distribution.

Land-use Conversions Predictors of Range Unfilling

Land-use intensification in the early stages of human societies' development negatively affects the species range unfilling globally. This relation, however, gradually changed and posted dramatic adverse effects on range unfilling since 1850 CE (Tab. 2). These results are consistent with our assumption that shifting from low or low-moderate to moderate land use could favor certain species to have greater occupancy of their potential ranges. In contrast, intensified land use after the era of discovery has progressively increased rang unfilling.

Indeed, land-use transformation in the early agriculture era is mainly characterized by conversing from wild and remote woodlands to populated and residential woodlands (1). Despite it being accompanied by extensive deforestation in some regions [Annex Fig. 17, (52, 53)], intensified human activities have helped certain tree species fill their potential ranges more (2). In the following agricultural era, inhabited drylands and remote woodlands are gradually declining with the replacement of a steady increment of intensive anthropomes, cultured anthropomes such as residential woodlands, and populated woodlands (1). An increase in tree cover and human activities reduces RU in this stage. This relation was continued for tree cover change in the coming era of discovery but started to have opposite effect between human activities and range unfilling. This

surprising change is related to the continuous increase of intensive anthromes (1). The land-use conversion was known as rapid industrialization and urbanization during the latest centuries (1, 54), with cultured anthromes and wildlands less than 50% of world land area today (1). Unfortunately, we found that this transition has significantly hindered the ability of tree species to occupy their potential ranges (Tab. 2).

Human activities have favored certain tree species to fill their potential range in the early stages, closely connected with all forms of utilization through propagation, domestication, and cultivation (2, 55). Indeed, the antagonistic relation between HM alteration and RU can be observed in all four testing realms in the early agricultural era (Tab. 3). However, the change of HM during the agricultural era in the Nearctic and Oceania does not follow this pattern (Tab. 3). This result perhaps is the product of colonization of woodlands and cultivated mosaic landscape due to the permanent indigenous settlements (56), which made the fire even more forceful than in Europe (57). On the other hand, range unfilling is not significantly influenced by tree cover change globally in the early agriculture era, owing to most land-use conversion happened in the Palearctic (Annex Fig. 17). The intensive deforestation in this biogeographic realm can be observed in our database for the EAE and AE (Annex Fig. 17 & 18), which has significantly hampered the possibility for tree species to extend their geographic ranges.

Conversely, both human pressure and tree cover alteration have positively impacted RU globally. These effects are evident in the Palearctic and Australasia for the EPFIR and EPSIR, respectively (Tab. 3). As an example, although tree cover had increased in some regions of the Palearctic with the replacement of inhabited drylands by intensive anthromes

during the EPFIR (1), it unfavored tree species to occupied their potential ranges (Tab. 3). Indeed, rapid industrialization and intensive land use are highly associated with species range contraction and extinction (58, 59).

Paleoclimate Anomaly Predictors of Range Unfilling

Our results show that the Miocene climate anomaly has little global impact on tree disequilibrium, whereas the LGM temperature anomaly negatively affected range unfilling. Despite the evident impact of Miocene precipitation anomaly in Palearctic and temperature anomaly in Neotropic, Afrotropic, and Indomalayan (Tab. 3), the limited global influence of the Miocene climate change could probably result from climate-driven regional extirpations (60, 61). Indeed, many endemic plant (woody) genera are restricted to some regions such as East Asia (62).

Significant impacts of LGM temperature anomaly can be observed in Australasia, Palearctic, and Oceania. This result matches with much empirical evidence that shows Quaternary climate anomalies have left legacies in current species distribution. An increasing number of large-scale studies of broad sets of European plant species have found that species' potential ranges were widely unfilled and, to some extent, still limited by the accessibility of recolonization from glacial refugia (14, 63). LGM climatic anomalies did not influence tree species distribution in Neotropic, Afrotropic, and Indomalayan, which is consistent with previous studies documenting that Quaternary climate change mainly has significant impacts in temperate regions of the Northern Hemisphere (3).

TABLE 3 Regression coefficients (showed confidence interval) of the relationship between predictors and range unfilling for seven major realms. The complete name of predictors can be found in Table 2. Continuous predictors were standardized to allow comparison. *** p < 0.001; ** p < 0.01; * p < 0.05.

	Neotropic	Afrotropic	Australasia	Indomalayan	Palaearctic	Nearctic	Oceania
TC		-0.13 ** [-0.23, -0.04]					-0.53 [-1.13, 0.08]
HM		0.04 [-0.05, 0.13]					
TC-EPSIR	0.01 [-0.04, 0.06]	-0.07 [-0.16, 0.02]	0.10 * [0.00, 0.19]	0.10 [-0.00, 0.19]	-2.40 *** [-3.48, -1.31]	0.36 ** [0.12, 0.59]	
HM-EPSIR	0.11 ** [0.04, 0.17]		0.32 *** [0.20, 0.43]	0.04 [-0.09, 0.17]		-0.26 [-0.61, 0.09]	
TC-EPFIR	-0.10 *** [-0.15, -0.04]	0.02 [-0.08, 0.13]	-0.04 [-0.16, 0.07]	0.00 [-0.13, 0.14]	1.52 *** [0.99, 2.04]	0.12 [-0.16, 0.40]	
HM-EPFIR	-0.11 ** [-0.18, -0.04]	-0.28 *** [-0.41, -0.15]	-0.28 *** [-0.45, -0.12]		2.27 *** [1.54, 3.00]	-0.05 [-0.25, 0.14]	0.01 [-0.38, 0.41]
TC-ED	-0.14 *** [-0.18, -0.09]	-0.09 ** [-0.15, -0.03]	0.16 [-0.04, 0.36]			0.29 [-0.05, 0.63]	0.10 [-0.17, 0.38]
HM-ED	0.03 [-0.03, 0.10]	-0.08 [-0.20, 0.04]	-0.36 *** [-0.55, -0.17]	-0.34 *** [-0.46, -0.21]	0.09 [-0.05, 0.24]		
TC-AE	-0.17 *** [-0.21, -0.12]	-0.02 [-0.11, 0.07]	-0.21 [-0.57, 0.15]	-0.07 [-0.18, 0.05]	-0.92 ** [-1.57, -0.28]	-0.22 [-0.46, 0.01]	
HM-AE			-0.03 [-0.21, 0.15]	-0.24 *** [-0.34, -0.13]	-0.87 [-2.18, 0.43]	0.25 * [0.04, 0.46]	0.39 * [0.03, 0.74]
TC-EAE	-0.06 * [-0.11, -0.01]	0.07 * [0.01, 0.13]	0.13 * [0.02, 0.24]		-1.97 *** [-2.71, -1.23]	-0.26 *** [-0.41, -0.12]	
HM-EAE	-0.24 *** [-0.31, -0.17]	-0.14 ** [-0.23, -0.06]	-0.02 [-0.13, 0.10]				-0.18 [-0.78, 0.43]
MAP	0.10 *** [0.06, 0.14]					-0.21 [-0.48, 0.07]	
MAT	-0.15 *** [-0.19, -0.10]	-0.22 *** [-0.35, -0.10]	0.08 [-0.07, 0.23]	-0.09 * [-0.16, -0.01]	-4.37 *** [-5.82, -2.92]	-0.07 [-0.33, 0.18]	
LGMPA	-0.02 [-0.06, 0.03]		-0.06 [-0.17, 0.04]	-0.05 [-0.13, 0.04]	4.01 *** [2.59, 5.44]	0.01 [-0.20, 0.22]	
LGMTA	0.01 [-0.03, 0.06]	-0.08 [-0.19, 0.04]	-0.13 ** [-0.22, -0.04]	0.04 [-0.06, 0.14]	-1.39 *** [-2.02, -0.75]	0.02 [-0.32, 0.36]	-0.81 ** [-1.39, -0.23]
MPA			-0.10 [-0.22, 0.03]	-0.03 [-0.12, 0.07]	2.02 *** [1.26, 2.77]		-0.37 [-0.87, 0.14]
MTA	-0.12 *** [-0.16, -0.07]	-0.22 *** [-0.32, -0.11]	-0.06 [-0.17, 0.05]	-0.25 *** [-0.35, -0.14]			
N	8924	3790	2943	1182	930	798	47
Pseudo R ²	0.03	0.03	0.03	0.11	0.31	0.09	0.43

Other Explanations

Other factors beyond land-use transformation and paleoclimate change could explain the findings. Indeed, even by including the difference of realms, these factors can only account for a 65.6% variance of range unfilling (Tab. 2). Noticeably, key ecological traits could also predispose certain species to fill their potential geographic range more. It is plausible that land-use conversion would directly or indirectly interact with the dispersal capacity of any given species by anthropogenic activities (55, 64). The utilization of (woody) plants for various purposes, including ornamental, food, and medicine, has significantly expanded their geographic ranges rather than unused contrast (2, 65). In addition, seed bank persistence, habitat breadth, and specific leaf area have also been associated with establishment and proliferation, which contributes to range limitations (66).

CONCLUSION

Our results suggest that global tree species are widespread unfilled, with species' potential ranges that have not been occupied 10.7 times larger than their geographic ranges. Regarding the uncertain sampling effort of the single dataset, future studies should incorporate diverse sources of occurrences records.

Data availability of global historical land-use conversions and paleoclimate changes is a major obstacle to understanding how past human activities and climate anomalies have shaped present-day species distribution. Here, our results show that the impacts of past human activities are significant globally by using the state-of-art database Anthromes (1), expanding our knowledge of prehistorical and historical land use in the current tree species distribution. Our results also show that LGM temperature anomaly negatively affects

range unfilling globally, leaving a significant mark in Australasia, Palearctic, and Oceania.

Our results highlight that the intensified human activities positively impacted current tree species distribution in the early eras of human society, whereas the opposite effects happened since the era of discovery. On the other hand, extensive deforestation has hampered tree species from filling their potential range more in the early stages. In contrast, the increase of tree cover during the post-industrial era, due to conversing from inhabitable drylands to intensive anthromes, has a positive effect on RU. This dramatic adverse effect of land-use conversion on tree species distribution within the last several hundred years should draw much attention to policymakers and conservationists to protect key biodiversity areas.

ACKNOWLEDGEMENTS

I sincerely thank my supervisor, Dr. Josep M. Serra-Diaz, for his invaluable guidance and support throughout the internship and for sharing his passion for ecological modeling with me. A special thank goes to AgroParisTech and Labex ARBRE. Without their financial support, I would not have had the opportunity to do this project. I am grateful for the valuable suggestions of R coding from Mr. Jeremy Borderieux and Mr. Arnaud Callebaut and the help standardizing species' taxonomic names from Ms. Julia Erbrech. I thank Dr. Gaspar Massiot for taking the time to answer my questions and sharing his knowledge about the generalized linear mixed model. I appreciate Dr. Jean-Claude Gégout for accepting to be my AgroParisTech academic tutor and for helping me when I needed it. Many thanks to my host laboratory UMR Ecosilva and all the incredible staff in the Rameau. I much enjoyed the peaceful and supportive working environment there.

REFERENCE

1. E. Ellis *et al.*, People have shaped most of terrestrial nature for at least 12,000 years. *Proceedings of the National Academy of Sciences* **118**, e2023483118 (2021).
2. C. Flower *et al.*, Human food use increases plant geographical ranges in the Sonoran Desert. *Global Ecology and Biogeography* **30**, 1461-1473 (2021).
3. J.-C. Svenning, W. L. Eiserhardt, S. Normand, A. Ordóñez, B. Sandel, The influence of paleoclimate on present-day patterns in biodiversity and ecosystems. *Annual Review of Ecology, Evolution, and Systematics* **46**, 551-572 (2015).
4. J. Rowan *et al.*, Geographically divergent evolutionary and ecological legacies shape mammal biodiversity in the global tropics and subtropics. *Proceedings of the National Academy of Sciences* **117**, 1559-1565 (2020).
5. C. Sirami *et al.*, Impacts of global change on species distributions: obstacles and solutions to integrate climate and land use: Land-use and climate change integration. *Global Ecology and Biogeography* **26**, (2016).
6. K. Donohue, D. R. Foster, G. Motzkin, Effects of the past and the present on species distribution: land-use history and demography of wintergreen. *Journal of Ecology* **88**, 303-316 (2000).
7. G. F. Ficetola *et al.*, Knowing the past to predict the future: land-use change and the distribution of invasive bullfrogs. *Global change biology* **16**, 528-537 (2010).
8. D. G. Gavin *et al.*, Climate refugia: joint inference from fossil records, species distribution models and phylogeography. *New Phytologist* **204**, 37-54 (2014).
9. M. Hermy, K. Verheyen, Legacies of the past in the present-day forest biodiversity: a review of past land-use effects on forest plant species composition and diversity. *Sustainability and diversity of forest ecosystems*, 361-371 (2007).
10. G. Tadesse, E. Zavaleta, C. Shennan, Effects of land-use changes on woody species distribution and above-ground carbon storage of forest-coffee systems. *Agriculture, ecosystems & environment* **197**, 21-30 (2014).
11. J. M. Serra-Díaz *et al.*, Disequilibrium of fire-prone forests sets the stage for a rapid decline in conifer dominance during the 21st century. *Scientific Reports* **8**, 1-12 (2018).
12. B. J. Seliger, B. J. McGill, J. C. Svenning, J. L. Gill, Widespread underfilling of the potential ranges of North American trees. *Journal of Biogeography* **48**, 359-371 (2021).
13. J. C. Svenning, F. Skov, Limited filling of the potential range in European tree species. *Ecology Letters* **7**, 565-573 (2004).
14. S. Normand *et al.*, Postglacial migration supplements climate in determining plant species ranges in Europe. *Proceedings of the Royal Society B: Biological Sciences* **278**, 3644-3653 (2011).
15. W. Xu *et al.*, Human activities have opposing effects on distributions of narrow-ranged and widespread plant species in China. *Proceedings of the National Academy of Sciences* **116**, (2019).
16. W.-Y. Guo *et al.*, High exposure of global tree diversity to human pressure. *Proceedings of the National Academy of Sciences* **119**, e2026733119 (2022).

17. K. J. Feeley, M. R. Silman, Land-use and climate change effects on population size and extinction risk of Andean plants. *Global change biology* **16**, 3215-3222 (2010).
18. J. Zhang *et al.*, Extinction risk of North American seed plants elevated by climate and land-use change. *Journal of Applied Ecology* **54**, 303-312 (2017).
19. A. Feurdean *et al.*, Biodiversity variability across elevations in the Carpathians: parallel change with landscape openness and land use. *The Holocene* **23**, 869-881 (2013).
20. E. Beech, M. Rivers, S. Oldfield, P. P. Smith, GlobalTreeSearch: The first complete global database of tree species and country distributions. *Journal of Sustainable Forestry*, (2017).
21. B. L. Boyle, Matasci, N., Mozzherin, D., Rees, T., Barbosa, G. C., Kumar Sajja, R., & Enquist, B. J. , I. B. I. a. E. Network., Ed. (<https://tnrs.biendata.org/> 2021).
22. S. Gaiji *et al.*, Content assessment of the primary biodiversity data published through GBIF network: status, challenges and potentials. *Biodiversity Informatics* **8**, (2013).
23. J. M. Serra-Diaz, B. J. Enquist, B. Maitner, C. Merow, J.-C. Svenning, Big data of tree species distributions: how big and how good? *Forest Ecosystems* **4**, 1-12 (2017).
24. A. Zizka *et al.*, CoordinateCleaner: Standardized cleaning of occurrence records from biological collection databases. *Methods in Ecology and Evolution* **10**, (2019).
25. A. Rabosky *et al.*, Coral snakes predict the evolution of mimicry across New World snakes. *Nature Communications* **7**, 11484 (2016).
26. M. Burgman, J. Fox, Bias in species range estimates from minimum convex polygons: Implications for conservation and options for improved planning. *Animal Conservation* **6**, (2003).
27. R. J. Hijmans *et al.*, Package ‘terra’. (2022).
28. K. Gaston, R. Fuller, The size of species' geographic ranges. *Journal of Applied Ecology* **46**, 1-9 (2009).
29. D. N. Karger *et al.*, Climatologies at high resolution for the earth's land surface areas. *Scientific Data* **4**, (2017).
30. B. Sandel *et al.*, The Influence of Late Quaternary Climate-Change Velocity on Species Endemism. *Science (New York, N.Y.)* **334**, 660-664 (2011).
31. M. Steinthorsdottir *et al.*, The Miocene: The Future of the Past. *Paleoceanography and Paleoclimatology* **36**, (2021).
32. M. Pound *et al.*, A Tortonian (Late Miocene, 11.61–7.25 Ma) global vegetation reconstruction. *Palaeogeography Palaeoclimatology Palaeoecology - PALAEOGEOGR PALAEOLIMATOL* **300**, 29-45 (2011).
33. M. Osman *et al.*, Globally resolved surface temperatures since the Last Glacial Maximum. *Nature* **599**, 239-244 (2021).
34. D. N. Karger, M. Nobis, S. Normand, C. Graham, N. Zimmermann, *CHELSA-TraCE21k v1.0. Downscaled transient temperature and precipitation data since the last glacial maximum.* (2021).
35. C. Kennedy, J. Oakleaf, D. Theobald, S. Baruch-Mordo, J. Kiesecker, Managing the middle: A shift in conservation priorities based on the global human modification gradient. *Global Change Biology* **25**, (2019).
36. M. C. Hansen *et al.*, High-Resolution Global Maps of 21st-Century Forest

- Cover Change. *Science (New York, N.Y.)* **342**, 850-853 (2013).
37. D. Baston, L. ISciences, M. D. Baston, Package ‘exactextractr’. *terra* **1**, 17 (2022).
38. J. Drake, Range bagging: A new method for ecological niche modelling from presence-only data. *Journal of the Royal Society, Interface / the Royal Society* **12**, (2015).
39. J. A. Hanley, B. McNeil, The Meaning and Use of the Area Under a Receiver Operating Characteristic (ROC) Curve. *Radiology* **143**, 29-36 (1982).
40. A. Hirzel, G. Lay, V. Helfer, C. Randin, A. Guisan, Evaluating the ability of habitat suitability models to predict species presences. *Ecological Modelling* **199**, 142-152 (2006).
41. T. Morelli *et al.*, The fate of Madagascar's rainforest habitat. *Nature Climate Change* **10**, 1-8 (2020).
42. P. E. McKight, J. Najab, Kruskal-wallis test. *The corsini encyclopedia of psychology*, 1-1 (2010).
43. C. Meyer, W. Jetz, R. P. Guralnick, S. A. Fritz, H. Kreft, Range geometry and socio-economics dominate species-level biases in occurrence information. *Global Ecology and Biogeography* **25**, 1181-1193 (2016).
44. B. Naimi, N. A. Hamm, T. A. Groen, A. K. Skidmore, A. G. Toxopeus, Where is positional uncertainty a problem for species distribution modelling? *Ecography* **37**, 191-203 (2014).
45. R. O'Brien, Dropping Highly Collinear Variables from a Model: Why it Typically is Not a Good Idea. *Social Science Quarterly* **98**, (2016).
46. J. P. Stevens, Outliers and influential data points in regression analysis.
- Psychological bulletin* **95**, 334 (1984).
47. R. C. Team, R: A language and environment for statistical computing. R Foundation for Statistical Computing, Vienna, Austria. <http://www.R-project.org/>, (2013).
48. M. L. de Araujo, A. C. Quaresma, F. N. Ramos, GBIF information is not enough: national database improves the inventory completeness of Amazonian epiphytes. *Biodiversity and Conservation*, 1-19 (2022).
49. W. K. Cornwell, W. D. Pearse, R. L. Dalrymple, A. E. Zanne, What we (don't) know about global plant diversity. *Ecography* **42**, 1819-1831 (2019).
50. A. Zizka *et al.*, No one-size-fits-all solution to clean GBIF. *PeerJ* **8**, e9916 (2020).
51. J. E. Pender *et al.*, How sensitive are climatic niche inferences to distribution data sampling? A comparison of Biota of North America Program (BONAP) and Global Biodiversity Information Facility (GBIF) datasets. *Ecological Informatics* **54**, 100991 (2019).
52. S. Bhagwat, C. Kettle, L. Koh, The history of deforestation and forest fragmentation: a global perspective. *Global forest fragmentation*, 5-19 (2014).
53. W. V. Harris, in *The Ancient Mediterranean Environment between Science and History*. (Brill, 2013), pp. 173-194.
54. R. Jedwab, D. Vollrath, Urbanization without growth in historical perspective. *Explorations in Economic History* **58**, 1-21 (2015).
55. C. Levis *et al.*, Persistent effects of pre-Columbian plant domestication on Amazonian forest composition. *Science* **355**, 925-931 (2017).

56. M. Williams, Dark ages and dark areas: global deforestation in the deep past. *Journal of historical geography* **26**, 28-46 (2000).
57. S. J. Pyne, F. I. America. (Princeton, NJ: Princeton University Press, 1982).
58. M. Konvicka, Z. Fric, J. Benes, Butterfly extinctions in European states: do socioeconomic conditions matter more than physical geography? *Global Ecology and Biogeography* **15**, 82-92 (2006).
59. M. Pacifici *et al.*, Global correlates of range contractions and expansions in terrestrial mammals. *Nature Communications* **11**, 1-9 (2020).
60. M. J. Donoghue, S. A. Smith, Patterns in the assembly of temperate forests around the Northern Hemisphere. *Philosophical Transactions of the Royal Society of London. Series B: Biological Sciences* **359**, 1633-1644 (2004).
61. M. J. Pound, A. M. Haywood, U. Salzmann, J. B. Riding, Global vegetation dynamics and latitudinal temperature gradients during the Mid to Late Miocene (15.97–5.33 Ma). *Earth-Science Reviews* **112**, 1-22 (2012).
62. S. R. Manchester, Z. D. CHEN, A. M. LU, K. Uemura, Eastern Asian endemic seed plant genera and their paleogeographic history throughout the Northern Hemisphere. *Journal of Systematics and Evolution* **47**, 1-42 (2009).
63. J. C. Svenning, F. Skov, Could the tree diversity pattern in Europe be generated by postglacial dispersal limitation? *Ecology letters* **10**, 453-460 (2007).
64. F. Della Rocca, P. Milanesi, Combining climate, land use change and dispersal to predict the distribution of endangered species with limited vagility. *Journal of Biogeography* **47**, 1427-1438 (2020).
65. R. Pouteau *et al.*, Climate and socio-economic factors explain differences between observed and expected naturalization patterns of European plants around the world. *Global Ecology and Biogeography* **30**, 1514-1531 (2021).
66. A. Estrada *et al.*, Species' intrinsic traits inform their range limitations and vulnerability under environmental change. *Global Ecology and Biogeography* **24**, 849-858 (2015).

ANNEX

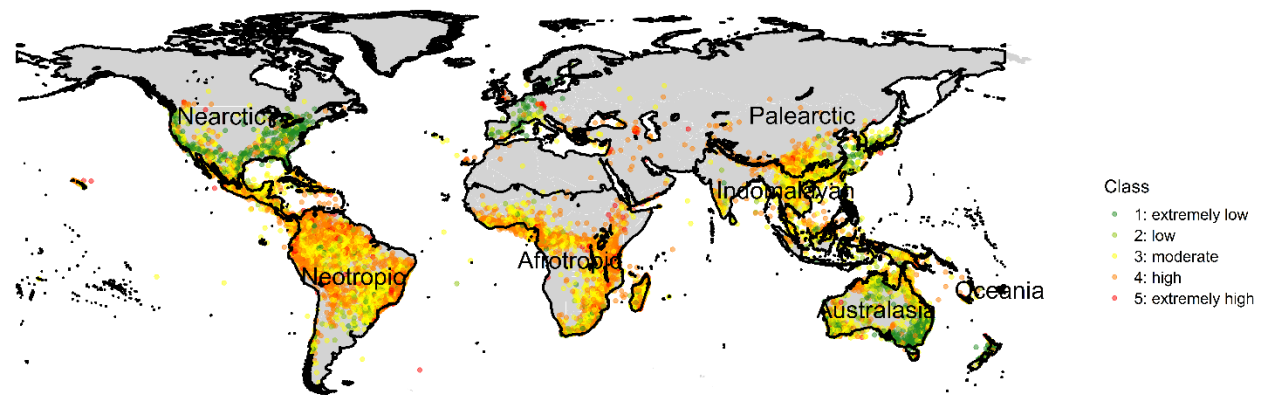


Figure 1 Global tree range unfilling map (showed in centroid). Range unfilling is showed in five classes: extremely low (class1, $0 < RU \leq 0.5$), low (class2, $0.5 < RU \leq 1$), moderate (class3, $1 < RU \leq 4$), high (class4, $4 < RU \leq 37$), extremely high (class5, $37 < RU$).

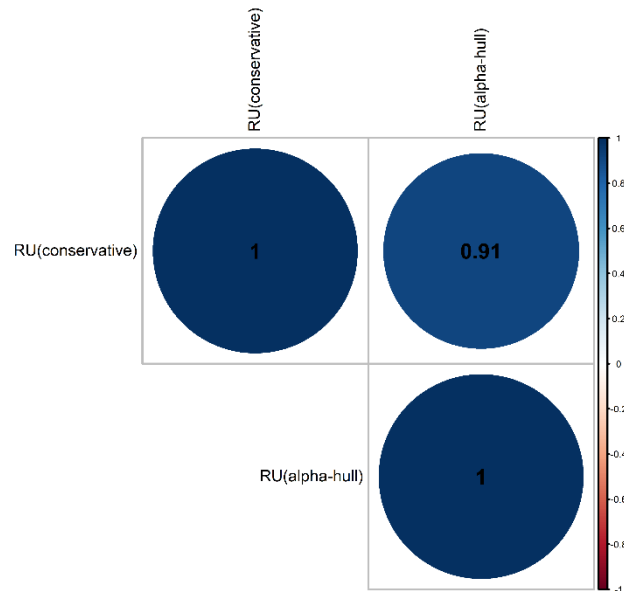


Figure 2 Pairwise correlation result of RU (conservative) and RU (alpha-hull). RU (conservative) is calculated as the ratio between the potential geographic range which has not (yet) been occupied and the estimated geographic range that overlapped with the potential range. RU (alpha-hull) is calculated as the ratio between the potential geographic range and the estimated geographic range.

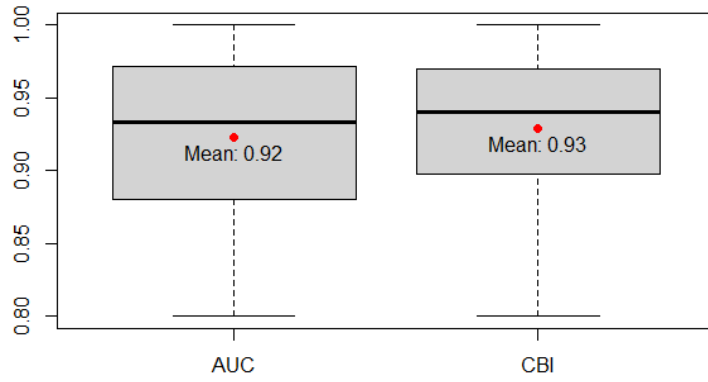


Figure 3 Distribution of AUC and CBI for SDMs which passed the model validation.

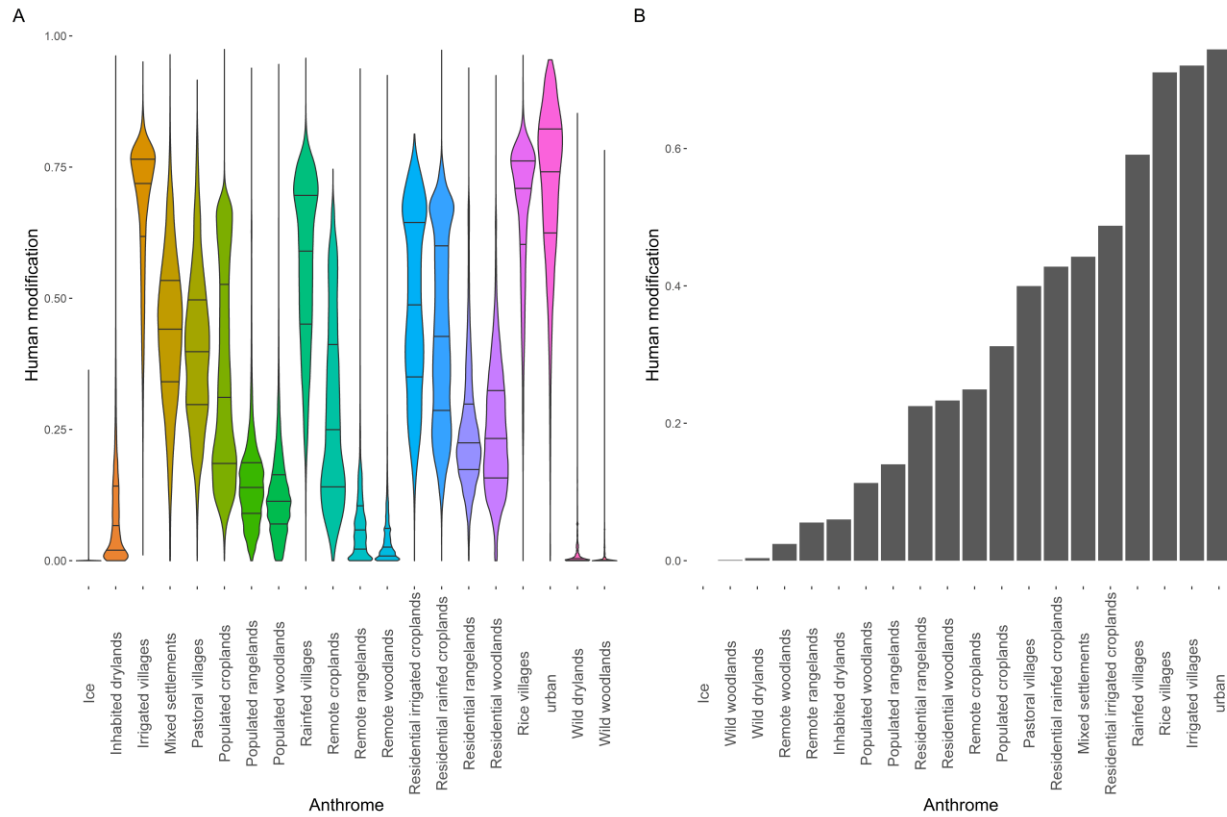


Figure 4 A. Variation of human pressure in the median year 2016, showed as human modification across anthromes. The result cannot be reordered owing to the limitations of the visualization package. B. Anthrome is reordered by the median value of human modification.

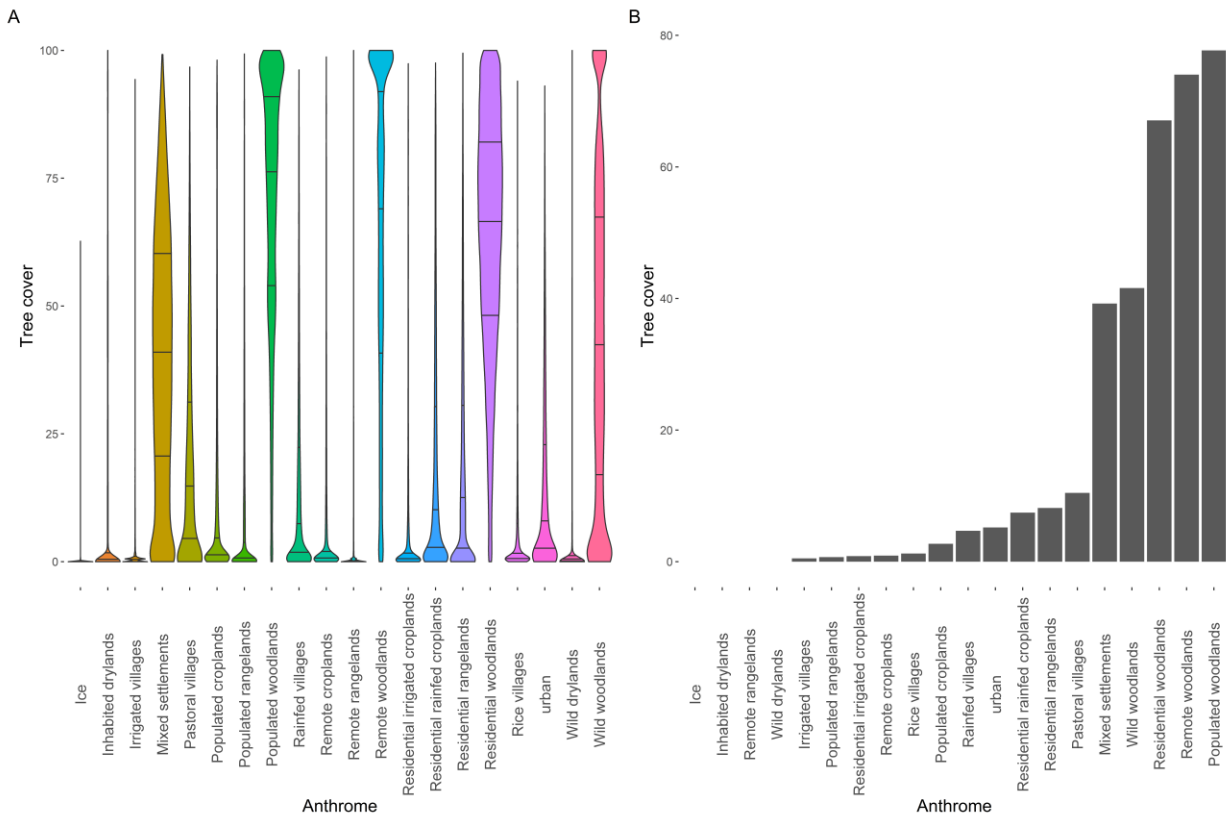


Figure 5 A. Variation of tree cover in 2010 across anthromes. The result cannot be reordered owing to the limitations of the visualization package. B. Anthrome is reordered by the median value of tree cover.

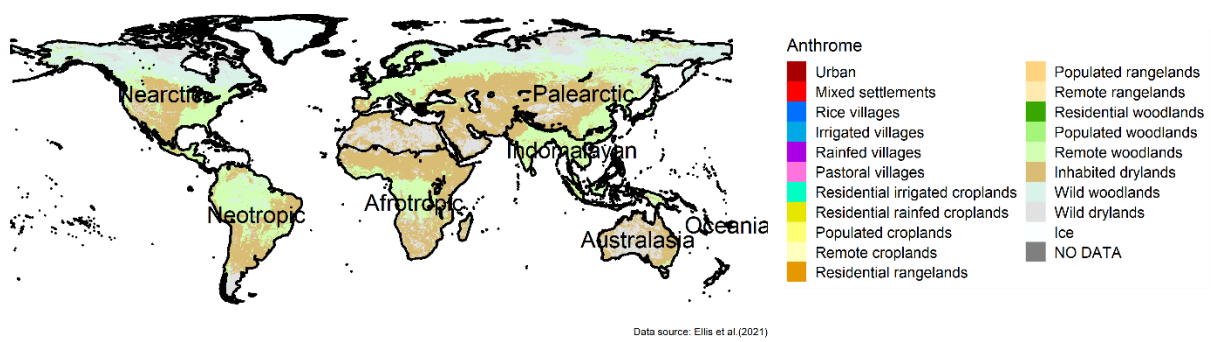


Figure 6 Global anthrome distribution in 10,000 BCE.

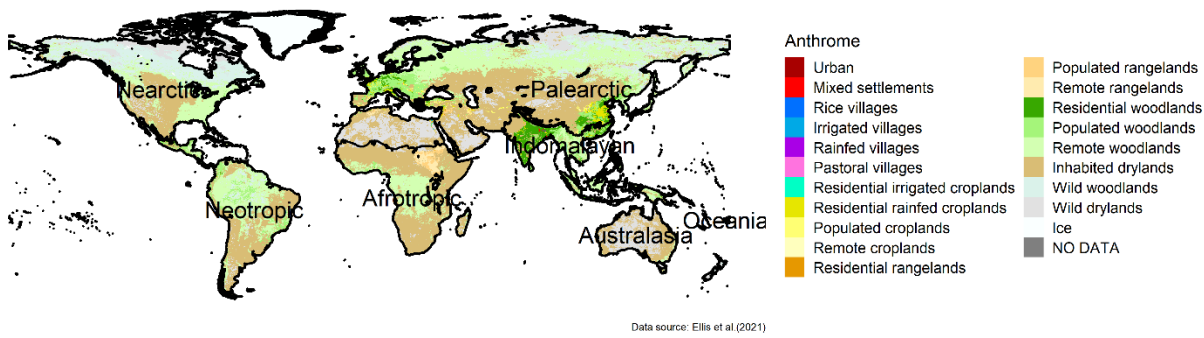


Figure 7 Global anthrome distribution in 1CE.

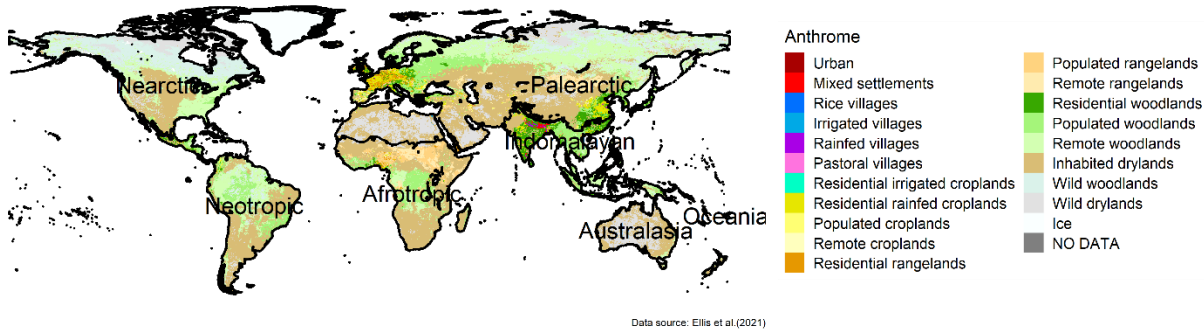


Figure 8 Global anthrome distribution in 1500CE.

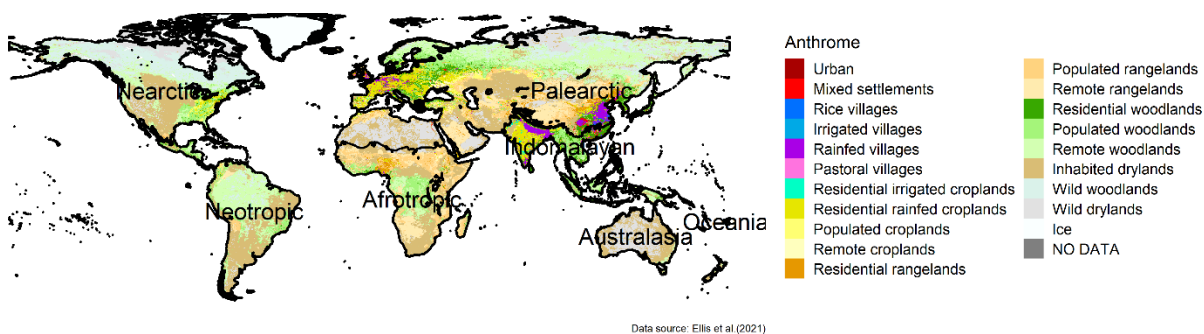


Figure 9 Global anthrome distribution in 1850CE.

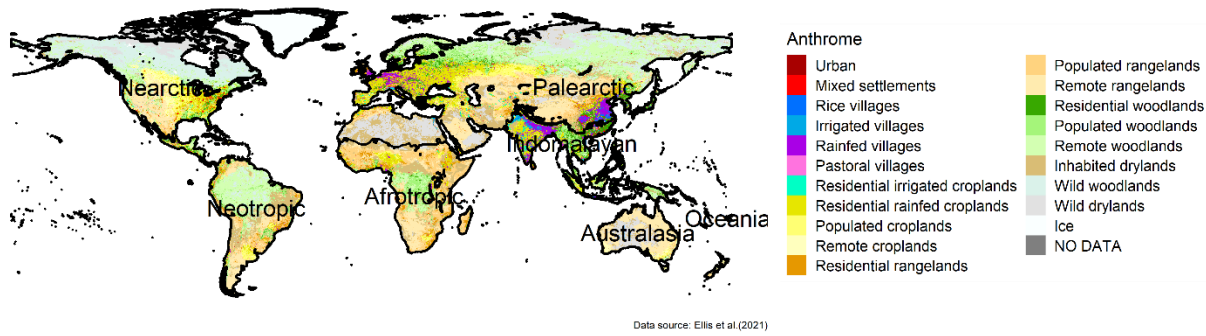


Figure 10 Global anthrome distribution in 1950CE.

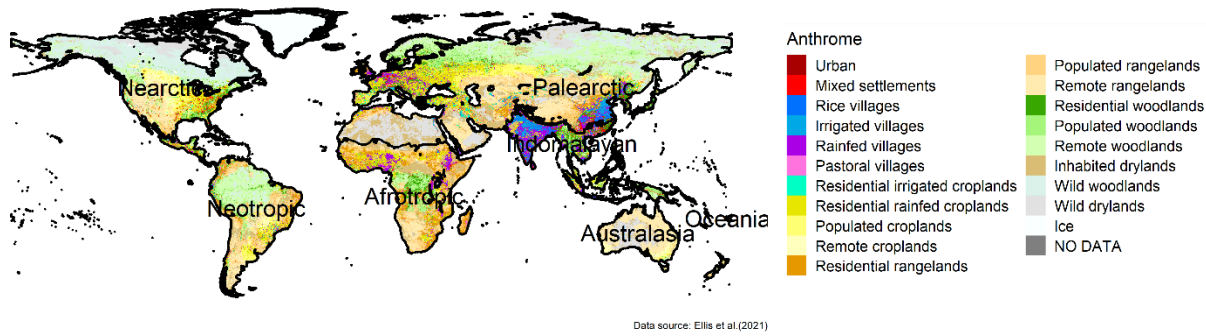


Figure 11 Global anthrome distribution in 2013CE.

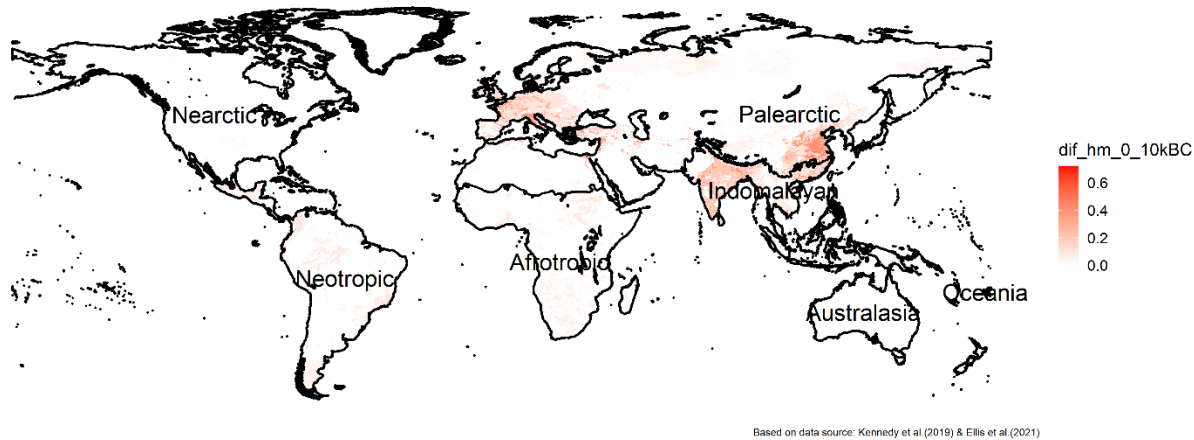


Figure 12 Global human pressure change during the early agricultural era.

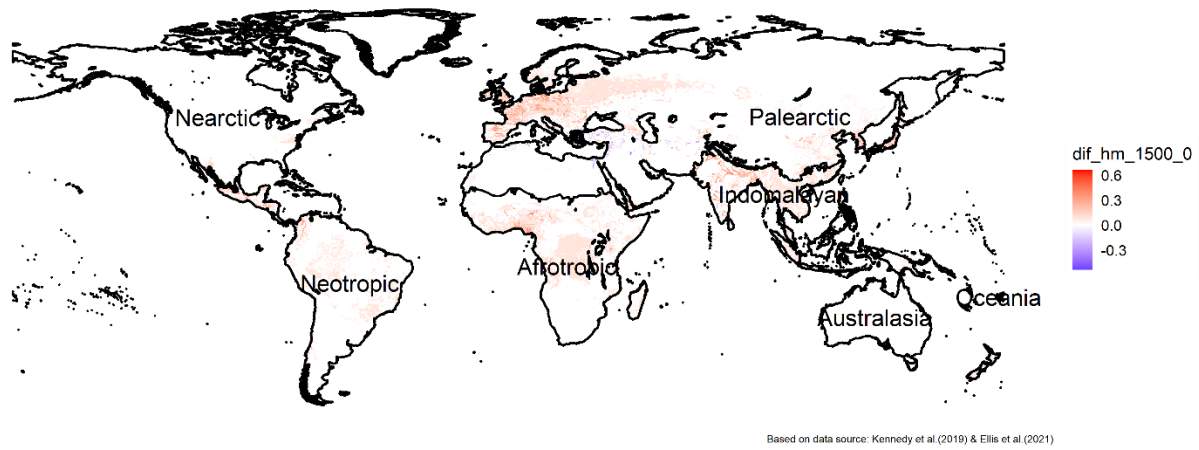


Figure 13 Global human pressure change during the agricultural era.

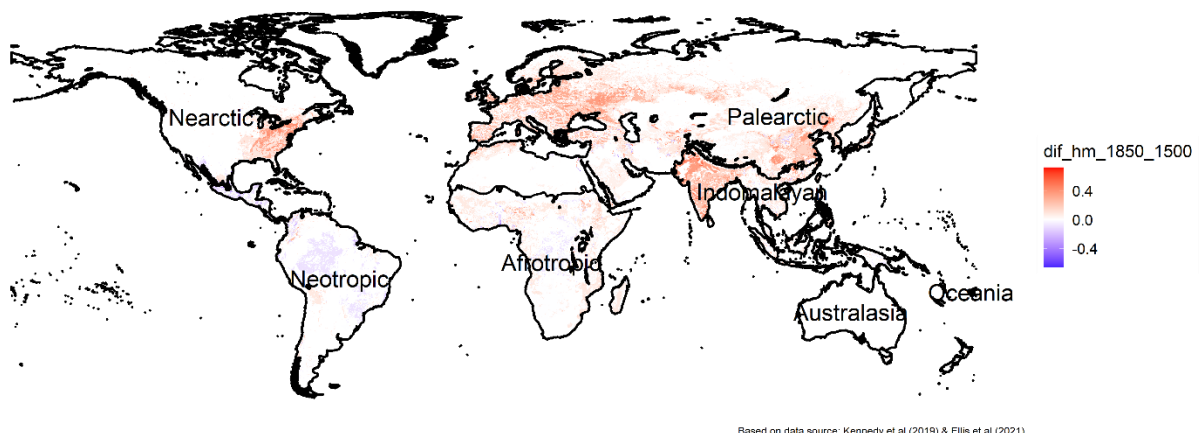


Figure 14 Global human pressure change during the era of discovery.

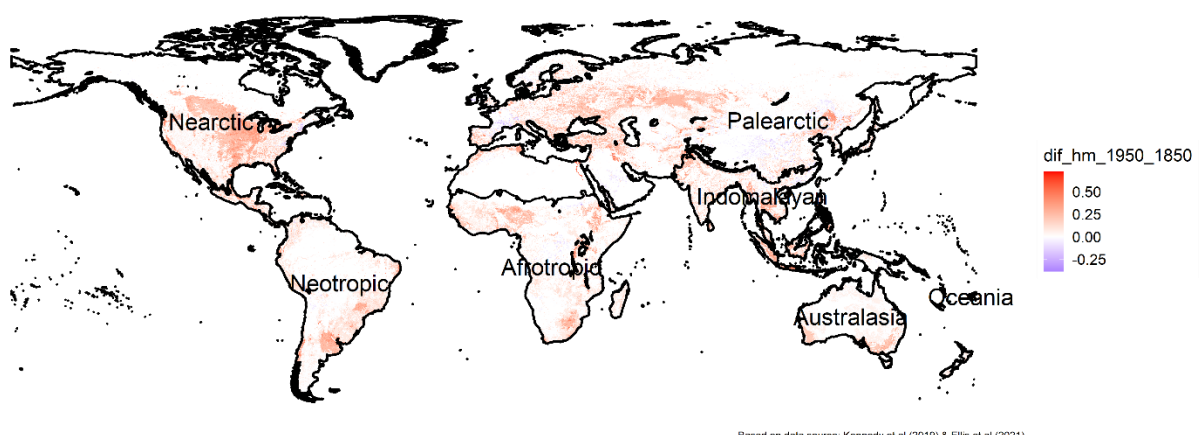


Figure 15 Global human pressure change during the era of post-first industrial revolution.

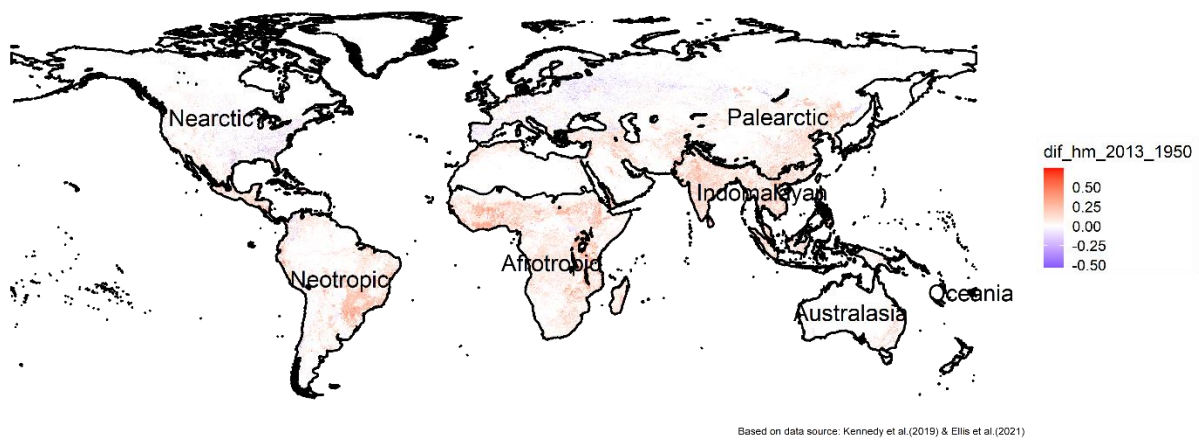


Figure 16 Global human pressure change during the era of post-second industrial revolution.

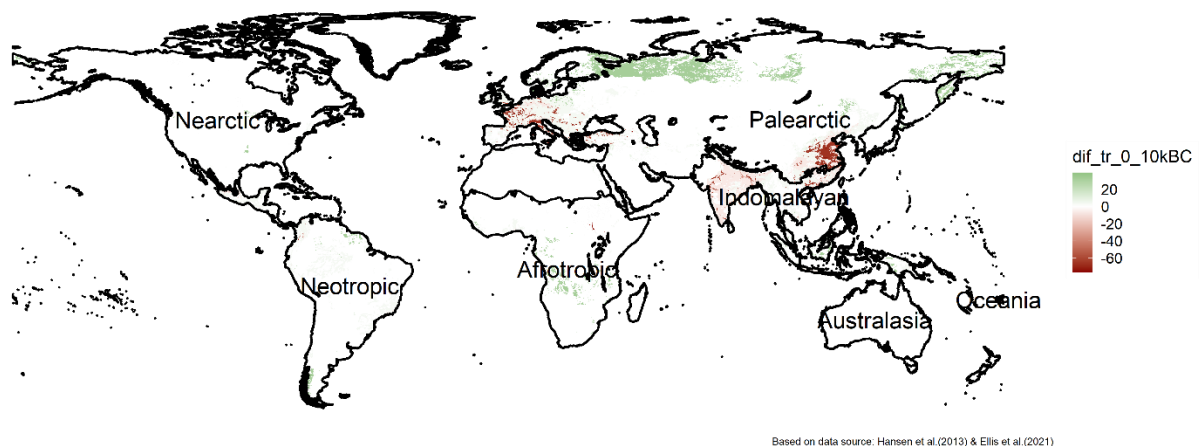


Figure 17 Global tree cover alteration during the early agricultural era.

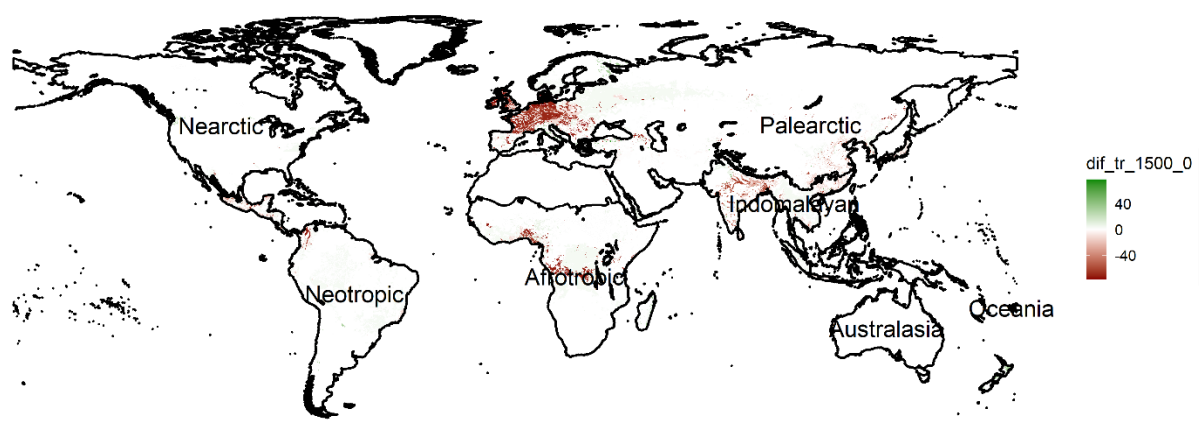


Figure 18 Global tree cover alteration during the agricultural era.

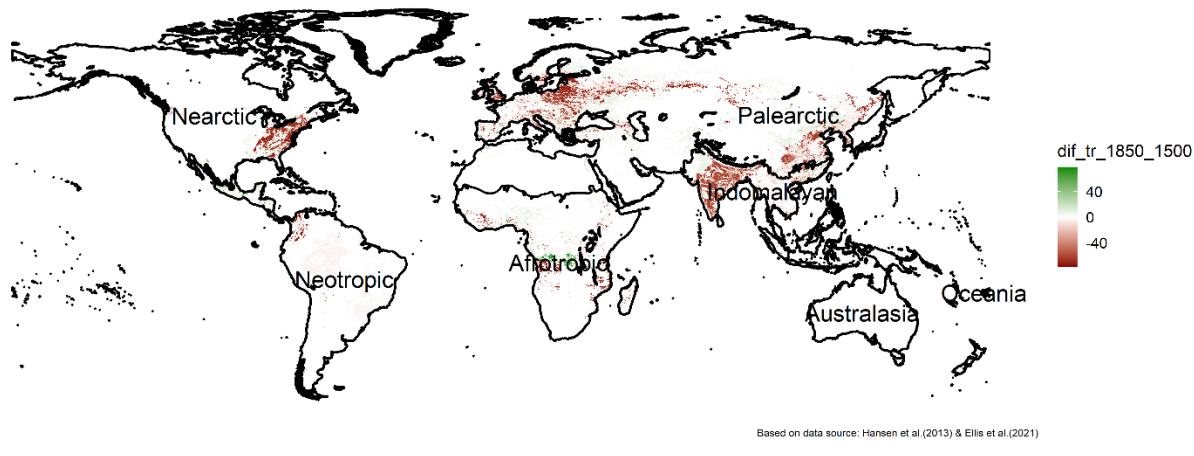


Figure 19 Global tree cover alteration during the era of discovery.

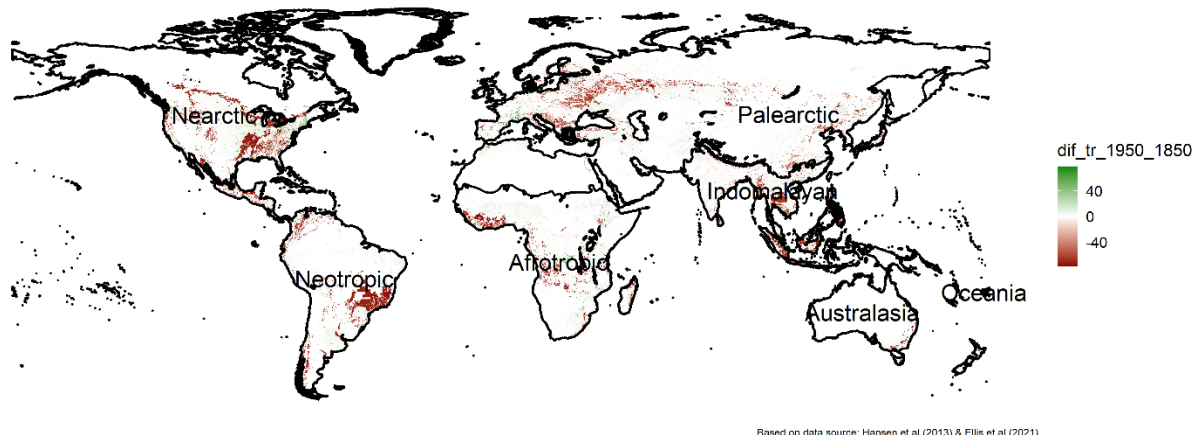


Figure 20 Global tree cover alteration during the era of post-first industrial revolution.

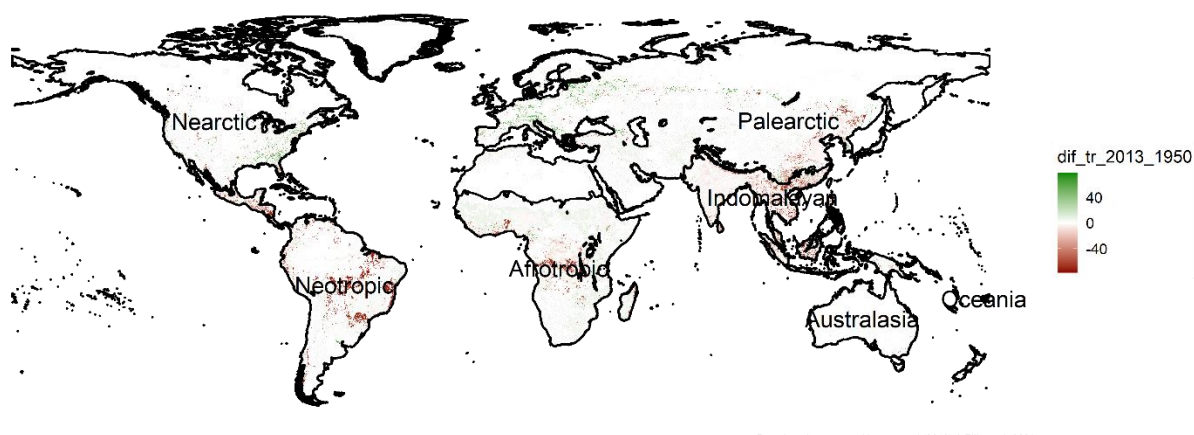


Figure 21 Global tree cover alteration during the era of post-second industrial revolution.

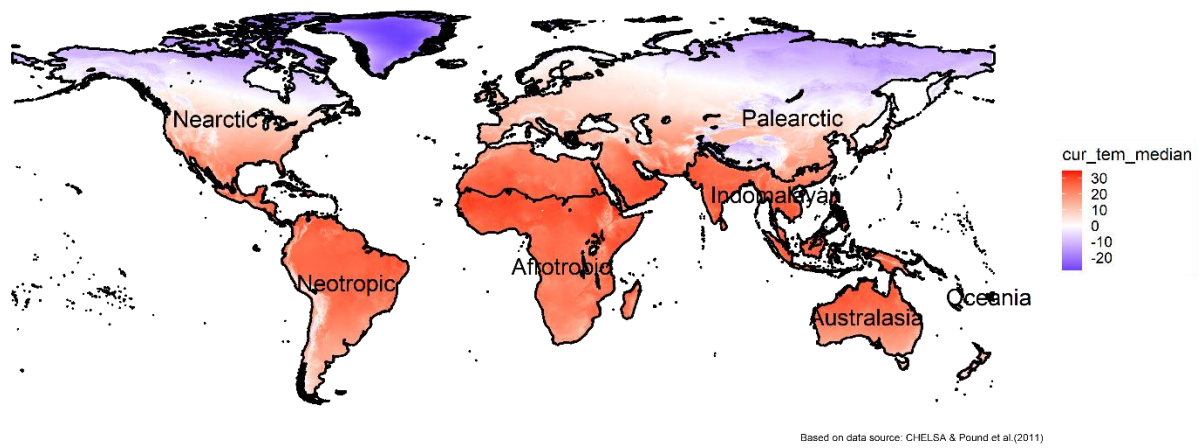


Figure 22 Global mean annual temperature from 1981 to 2010.

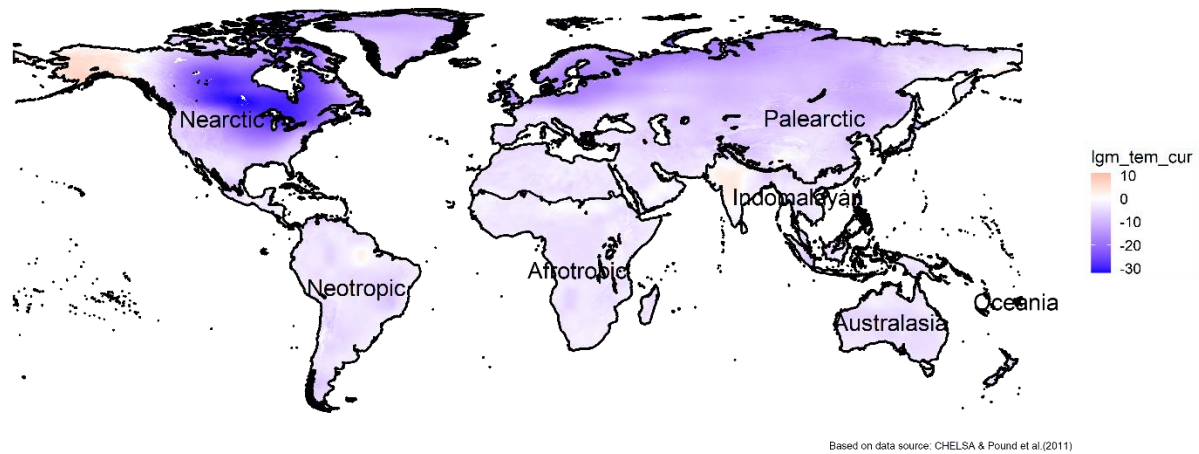


Figure 23 Global Last Glacial Maximum temperature anomaly.

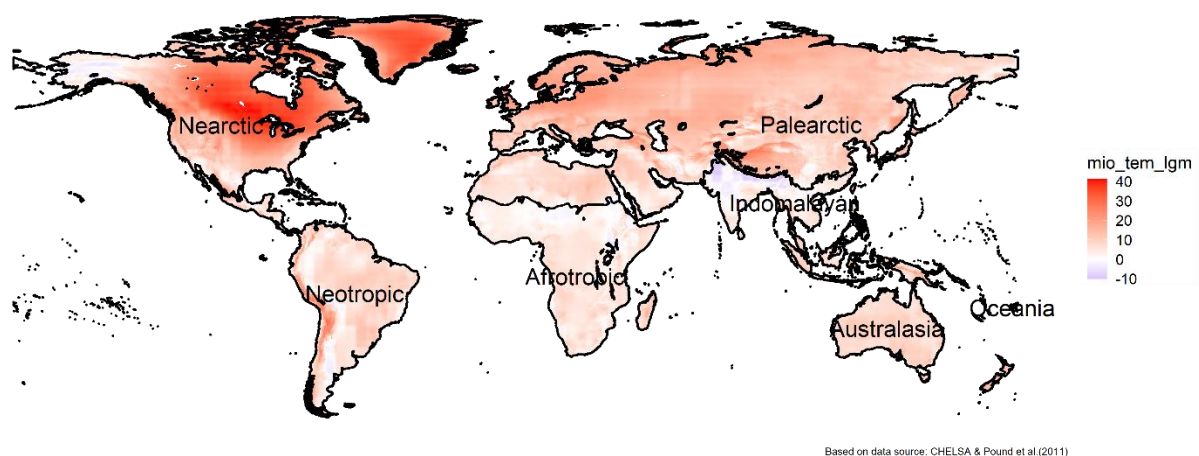


Figure 24 Global Miocene temperature anomaly.

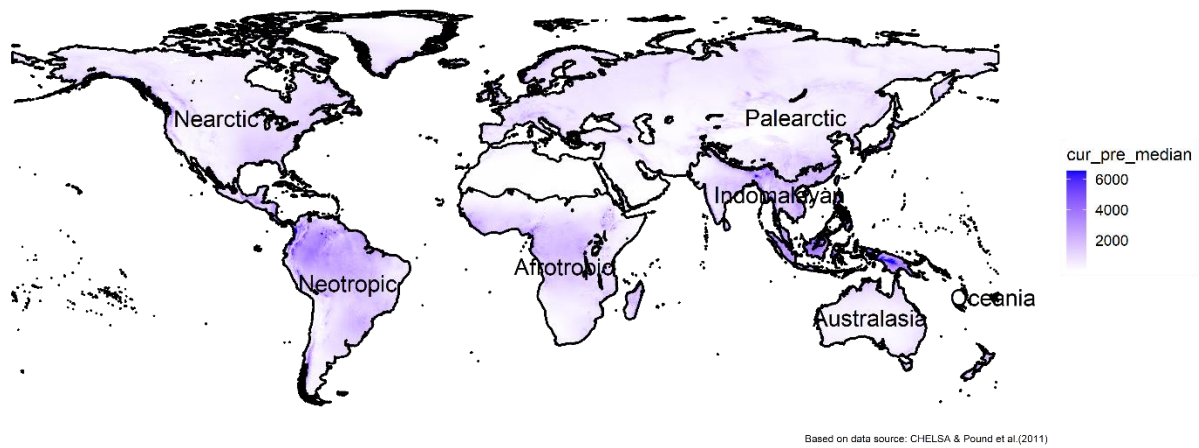


Figure 25 Global mean annual precipitation from 1981 to 2010.

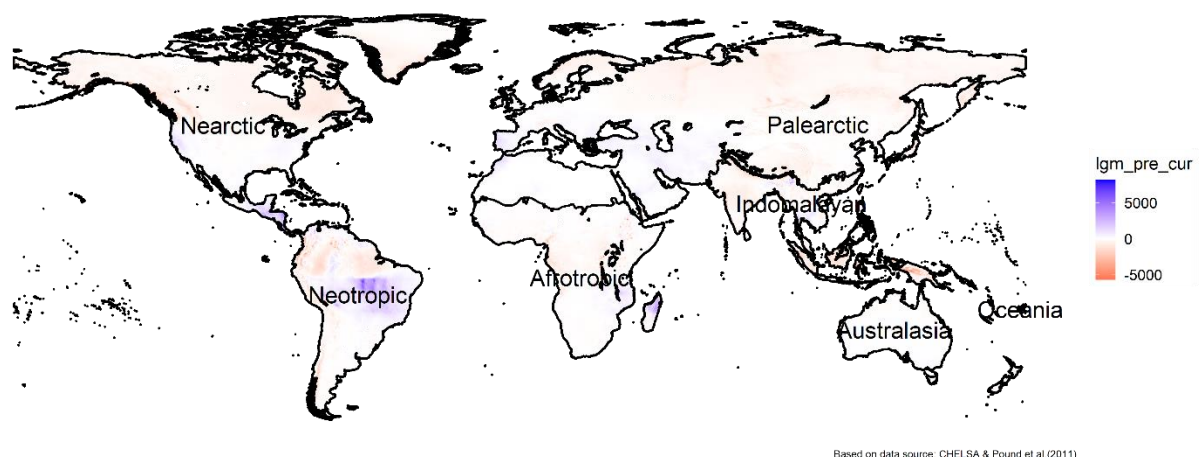


Figure 26 Global Last Glacial Maximum precipitation anomaly.

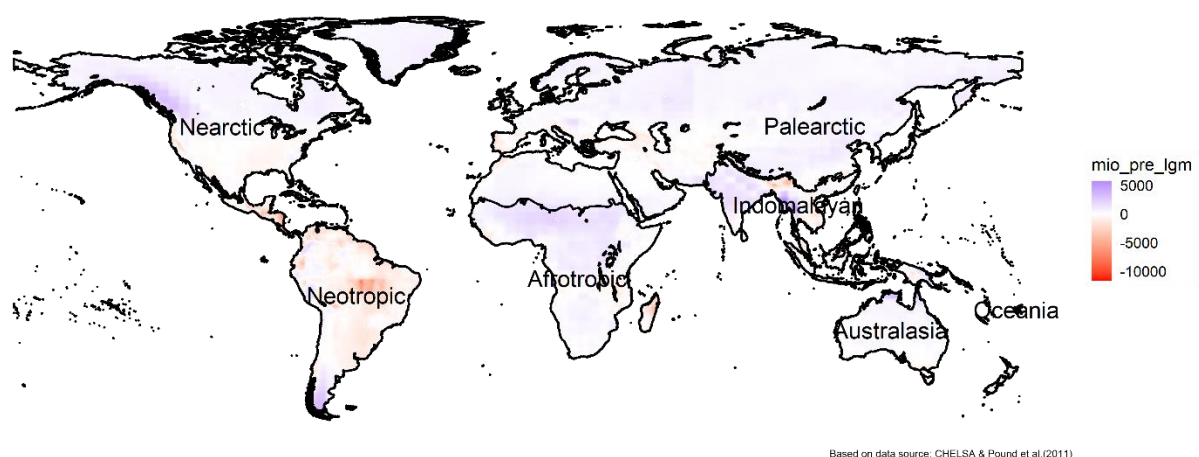


Figure 27 Global Miocene precipitation anomaly.

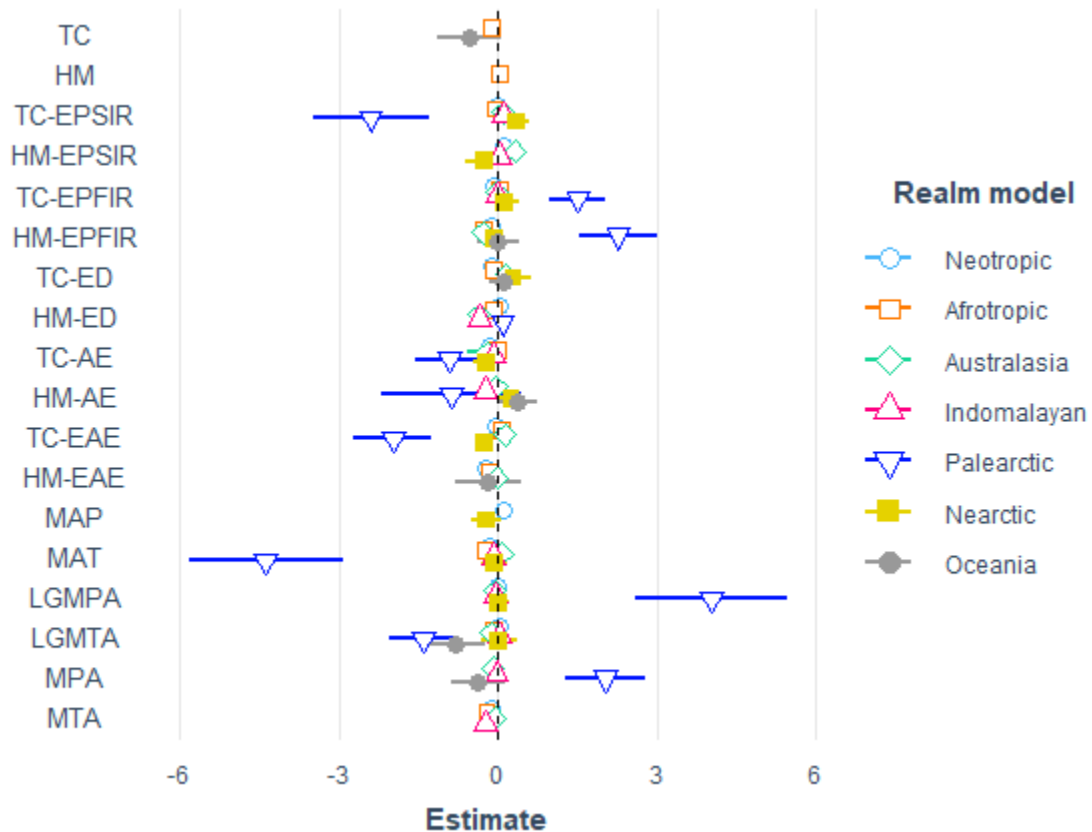


Figure 28 Regression coefficients of the relationships between predictors and range unfilling across seven major realms. Coefficients (estimates) showed with confidence interval. Continuous predictors were standardized to allow comparison. The complete name of predictors can be found in Table 2.